SGSMP
SSRPM
SSRFM

Schweizerische Gesellschaft für Strahlenbiologie und Medizinische Physik
Société Suisse de Radiobiologie et de Physique Médicale
Società Svizzera di Radiobiologia e di Fisica Medica
Swiss Society of Radiobiology and Medical Physics

56th SSRMP Annual Meeting

30.11. / 01.12.2023

Verkehrshaus der Schweiz, Lucerne

Booklet

Thank you to our generous corporate supporters

Accuray International SARL
Aquilab
Brainlab Sales GmbH
Conmedica GmbH
Limbus AI / Irudigi
medisynt / Solumedics
Meditron SA / RTI Group
MIM Software Inc.
MVision AI / Staila Polaris
PTW Freiburg GmbH
Qualiformed SARL
Raditec Medical AG
Vision RT GmbH

Conference Center (Verkehrshaus der Schweiz)

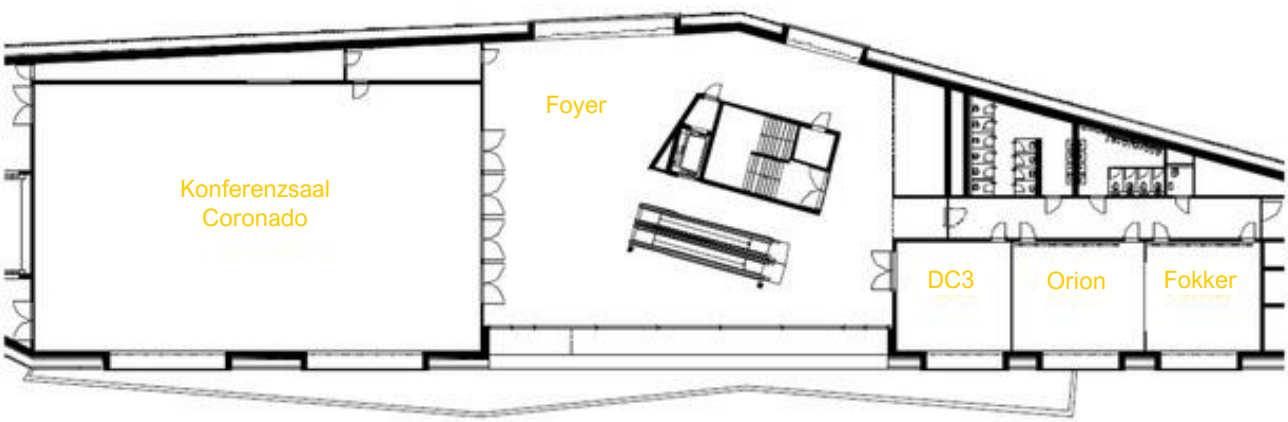

Foyer (Conference Center)

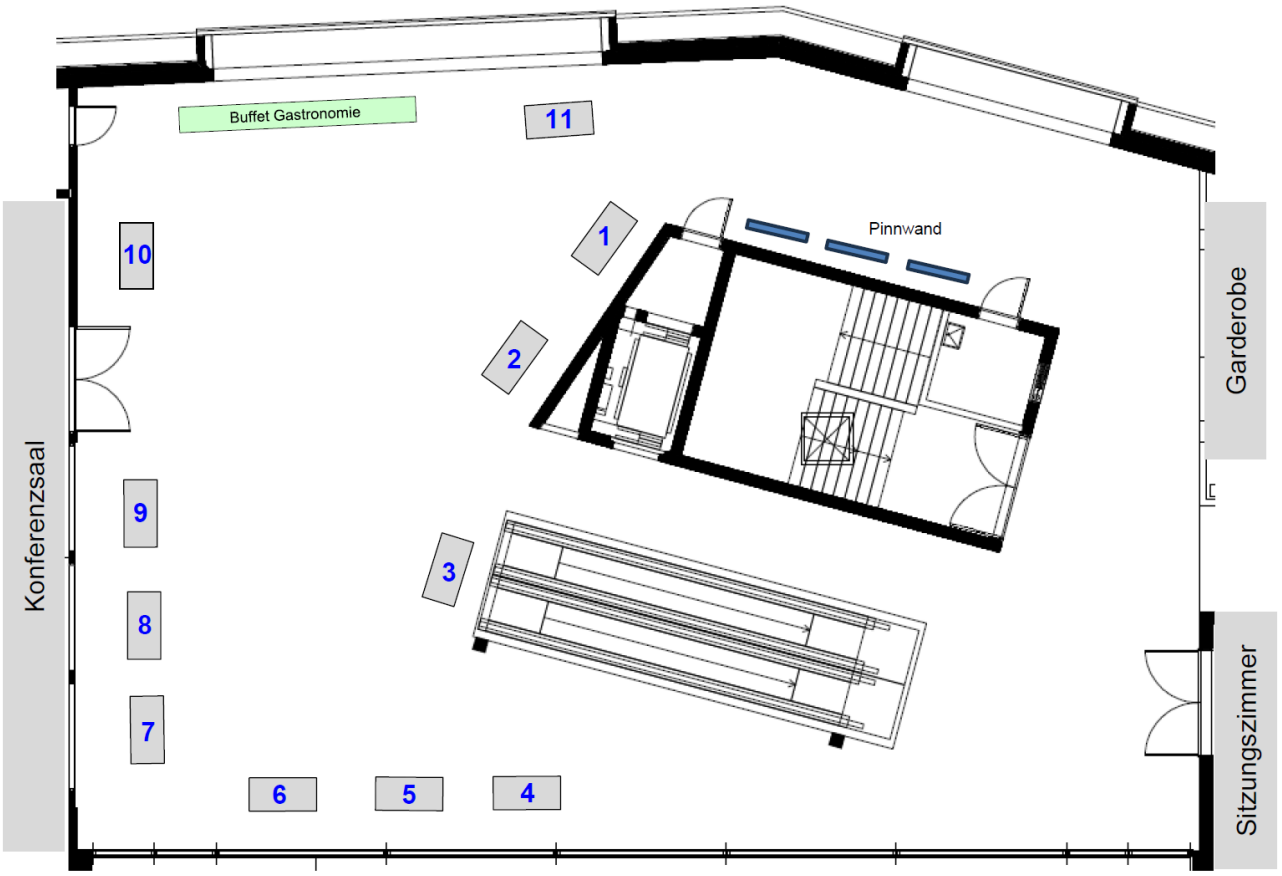

12	Accuray International SARL	1	medisynt / Solumedics	5	Raditec Medical AG
13	Aquilab	15	Meditron SA / RTI Group	3	Sun Nuclear GmbH
16	Brainlab Sales GmbH	11	MIM Software Inc.	2	Varian / Siemens Healthineers International AG
7	Conmedica GmbH	14	MVision AI / Staila Polaris		
9	Elekta GmbH	10	PTW Freiburg GmbH	4	Vision RT GmbH
6	Limbus AI / Irudigi	8	Qualiformed SARL		

Sitzungszimmer (Conference Center)

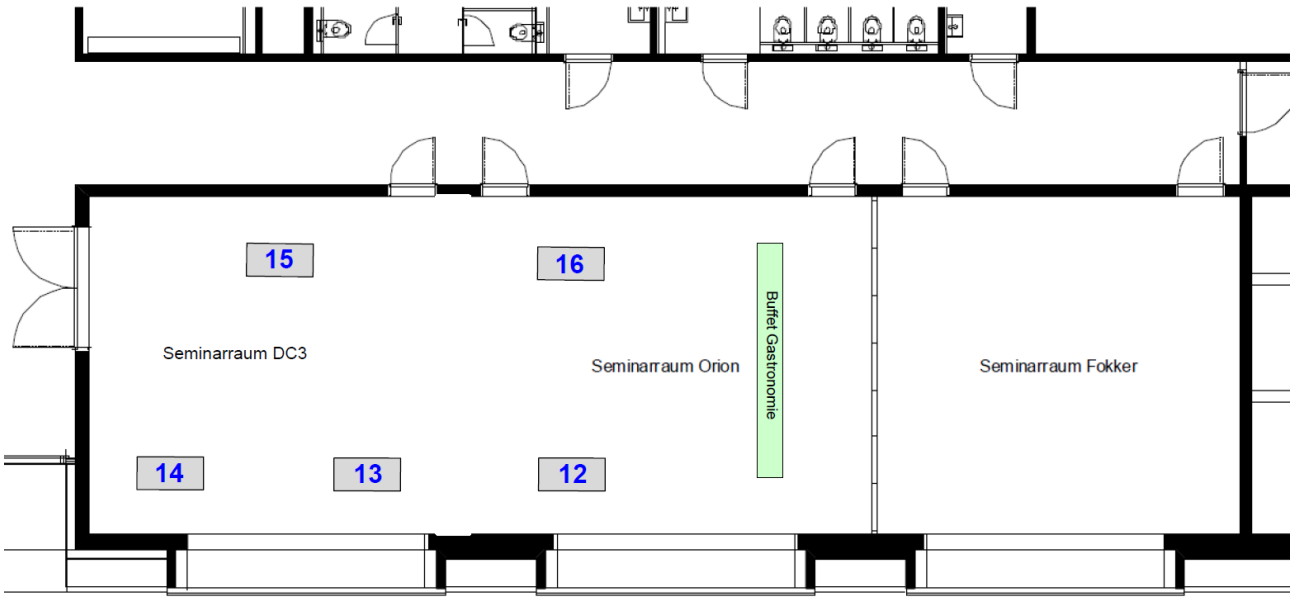

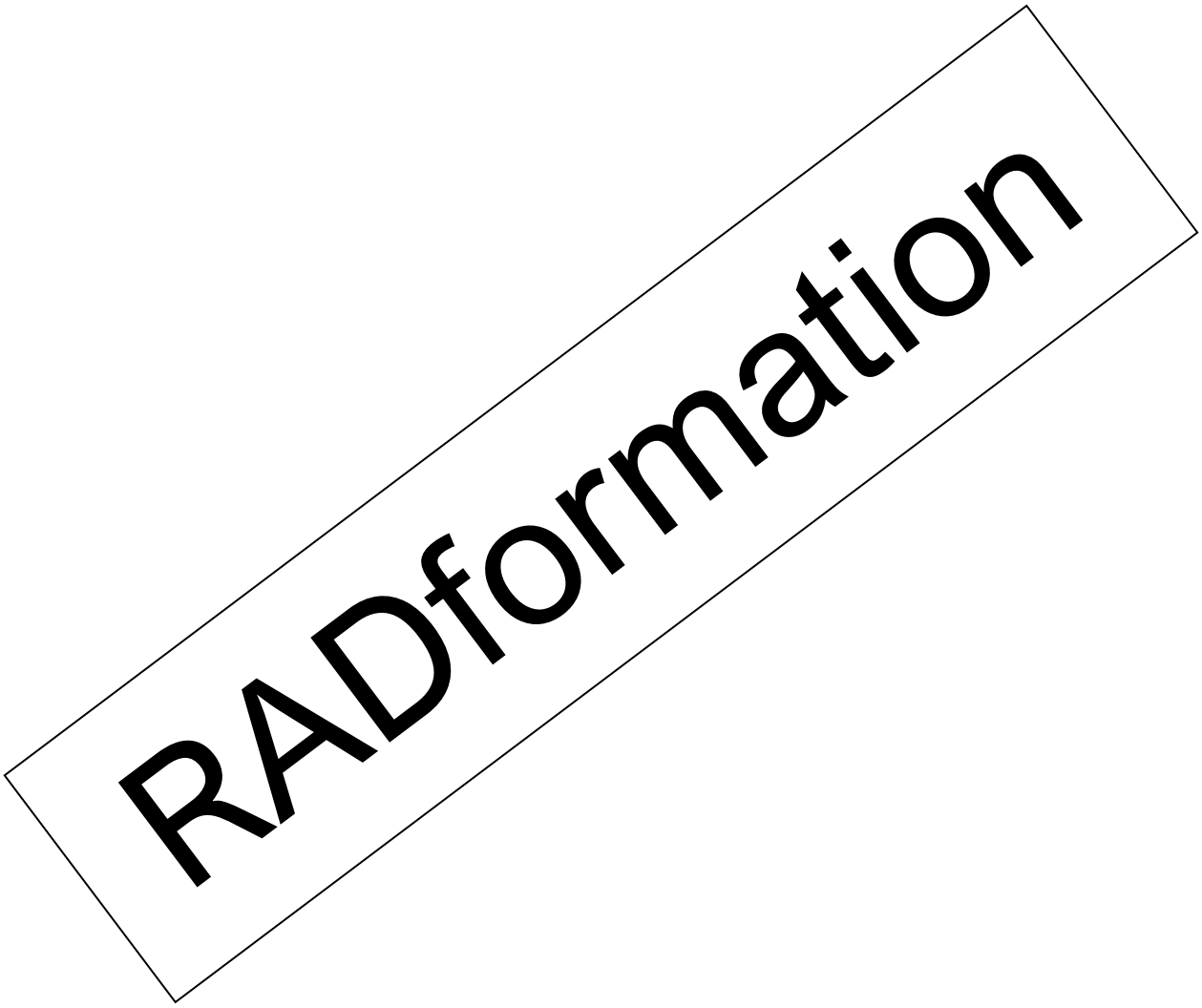
RADformation

Timetable

Thursday, 30 November 2023

09:00 – 10:00	Registration
10:00 – 10:10	Opening
10:10 – 10:40	SSRMP Research Grant *Chair: Maud Jaccard*
10:40 – 11:40	Session I: Nuclear Medicine, Radiation Protection & Radiobiology *Chair: Lorenzo Mercolli, Thiago Lima*
11:40 – 13:10	Lunch & Industry
13:10 – 14:40	Session II: Radiation Oncology *Chair: Chengchen Zhu*
14:40 – 15:10	Coffee Break & Industry
15:10 – 15:40	Invited Speaker: Dr. Marta Cremonesi Molecular radiotherapy and external beam radiation therapy: to date applications and future views *Chair: Silvano Gnesin*
15:40 – 17:00	SSRMP General Assembly
17:00 – 18:00	Planetarium Phantom of the Universe: The hunt for dark matter has begun
18:30 – 22:00	Social Event - Apéro and Dinner Schiffrestaurant Wilhelm Tell

Friday, 1 December 2023

09:00 – 10:10	Session III: Radiation Oncology *Chair: Hannes A. Loebner*
10:10 – 10:40	Coffee Break & Industry
10:40 – 11:30	Session IV: Diagnostics *Chair: Nick Rykx, Natalia Saltybaeva*
11:30 – 13:00	Lunch & Industry
13:00 – 13:30	Invited Speaker: Dr. Javier Montoya Cracking the code: demystifying AI in medical imaging *Chair: Milena Gravinatti*
13:30 – 14:40	Session V: Radiation Oncology *Chair: Florian Amstutz*
14:40 – 15:10	Coffee Break & Industry
15:10 – 15:50	Session VI: Radiation Oncology *Chair: Tino Streller*
15:50 – 16:00	Closing

Contributions

Session I: Nuclear Medicine, Radiation Protection & Radiobiology		
10:40 – 10:50	Siria Medici	Medical physics support for protocol optimization in PET and SPECT: a survey
10:50 – 11:00	Silvano Gnesin	Quantitative accuracy of Y-90-microspheres vial activities, results from PET experiments and Monte Carlo simulations
11:00 – 11:10	Milena Cristina Gravinatti	Impact of reconstruction parameters in Luthetium-177 dosimetry
11:10 – 11:20	Davide Cester	Initial experience with dedicated eye lens dosimetry in interventional radiology
11:20 – 11:30	Tristan Genetay	Assessment of radiation dose values for fluoroscopy examinations in the operating theatre
11:30 – 11:40	Verdiana Trappetti	Microbeam radiation therapy: the next generation GRID-RT

Session II: Radiation Oncology		
13:10 – 13:20	Daniel Hosie	Modelling the biological effect of temporally feathered radiotherapy
13:20 – 13:30	Lukas Wissmann	RT-EQD2: a tool for 3D evaluation of biologically weighted dose estimates
13:30 – 13:40	Vivek Maradia	Revolutionizing particle therapy: a compact and cost-effective cyclotron-based proton facility
13:40 – 13:50	Keegan McNamara	First in-beam measurements of a multi-field proton treatment plan with the open-ring PETITION scanner
13:50 – 14:00	Lisa Stefanie Fankhauser	A comprehensive analysis of RBE uncertainties and their potential clinical consequences for head and neck cancer
14:00 – 14:10	Isabella Colizzi	Comprehensive exploration of beam size and divergence variations in proton therapy facilities
14:10 – 14:20	Gian Guyer	Direct aperture optimization-based pathfinding for non-isocentric dynamic trajectory radiotherapy applied to a craniospinal irradiation case
14:20 – 14:30	Annalisa Walpen	Comparison of geometric and dosimetric-based path-finding for dynamic collimator-radiotherapy (colli-DTRT)
14:30 – 14:40	Alina Paunoiu	Robust dynamic-collimator trajectory radiotherapy (colli-DTRT)

Session III: Radiation Oncology		
09:00 – 09:10	Renato Bellotti	JulianA: automatic spot weight optimisation for proton radiotherapy
09:10 – 09:20	Daniel Björkman	Impact of penumbra sharpness on lateral margin requirement for ocular proton therapy
09:20 – 09:30	Anne zur Horst	Tissue assignment using combined MR CT for activation calculations in pencil beam scanning proton therapy patients
09:30 – 09:40	Martina Bonomi	Improving proton therapy delivery efficiency via combination of advanced spot positioning algorithms and ridge filter
09:40 – 09:50	Marie Fargier-Voiron	Synchrony modality on Radixact: evaluation of the targeting accuracy
09:50 – 10:00	Maude Gondré	Robust optimization of lung SBRT treatments using CyberKnife with Synchrony and X-Sight Spine tracking methods
10:00 – 10:10	Peter Peier	Reference dosimetry for electron FLASH radiotherapy at METAS

Session IV: Diagnostics		
10:40 – 10:50	Laura Dupont	Influence of age and breast density on the radiation dose received for a mammography examination
10:50 – 11:00	Anais Viry	Optimization of CT pulmonary angiography using task-based image quality assessment and diagnostic reference levels: An example of the implication of medical physicists in CT
11:00 – 11:10	Damien Racine	Integrating temporal resolution on the non-prewhitening model observer in computed tomography
11:10 – 11:20	Elina Samara	Patient eye lens radiation exposure during interventional neuroradiology procedures
11:20 – 11:30	David Stocker	Probabilistic U-Net model observer for the DDC method in CT scan protocol optimization

Session V: Radiation Oncology		
13:30 – 13:40	Michele Zeverino	Adaptation of left-sided breast deep learning auto-planning model for right-sided breast treatments
13:40 – 13:50	Raphael Joost	DeepSMCP – deep-learning powered denoising of MC dose distributions
13:50 – 14:00	Katerine Viviana Diaz Hernandez	Quality assessment of automatically planned O-Ring linac SBRT plans for lung metastases, evaluating the optimal minimum target size
14:00 – 14:10	Nathan Torelli	Dosimetrically motivated collimator angle optimization for linac-based stereotactic radiosurgery of multiple brain metastases
14:10 – 14:20	Florian Dietsche	Development of a workflow to upload treatment plans generated with a research TPS into the commercial Eclipse TPS
14:20 – 14:30	Beiqian Qi	Quality assurance for implementation of online adaptive radiotherapy
14:30 – 14:40	Katarzyna Czerska	Failure modes and effects analysis of the daily adaptive proton therapy workflow at PSI

Session VI: Radiation Oncology		
15:10 – 15:20	Björn Zobrist	Monte Carlo dose calculation for moving and deforming anatomy
15:20 – 15:30	Michael Fix	Monte Carlo model of an ETHOS radiotherapy beam
15:30 – 15:40	Francine El Khoury Youhanna	Validation of a 6 MV flattening filter free phase space of a C-arm linear accelerator for a Monte Carlo framework
15:40 – 15:50	Chengchen Zhu	Monte Carlo codes for very high energy electrons: dosimetric and calculation time comparison

Poster Presentation:		
	Konstantinos Zeimpekis	Post Y-90 radioembolization patient image quality and dosimetry evaluation with whole-body Biograph Quadra PET/CT


QualiFormeD

Medical physics support for protocol optimization in PET and SPECT: a survey

Siria Medici[1], Silvano Gnesin[1]

[1]*Institute of Radiation Physics, Lausanne University Hospital, Lausanne*

Purpose

The Swiss Radiological Protection Ordinance stipulates that medical physicists should be involved in the optimization of clinical protocols. We present a multicentric and multidevice study to evaluate the impact of protocol optimization on image quality (IQ) in nuclear medicine.

Methods

We performed a NEMA phantom study in 15 centres mainly located in western Switzerland, for a total of 17 SPECT and 10 PET devices. The phantom was either filled with Tc-99m or F-18 and the activity concentration was representative of the one encountered in the clinics for bone SPECT and oncologic FDG for PET. The activity concentration ratio between hot spherical inserts and homogeneous background was 10:1. The administered activity in each centre was compared to the national dose reference levels (DRL) and the calibration accuracy of quantitative systems was verified.

The IQ was assessed through the coefficient of variation (COV in homogeneous background), contrast to noise ratio (CNR), hot and cold contrast and recovery coefficients (RC) in spherical inserts.

The IQ between original and optimized protocols was compared. The influence of acquisition (scan duration) and reconstruction parameters (iterative updates and post-processing filtering) were assessed.

Results

Important improvements in the hot contrast (up to +80%) and cold contrast could be achieved by adjusting reconstruction parameters, at the cost of an increase of image noise in the phantom background.

For quantitative devices, the percent difference between the measured and the true activity concentrations in the phantom background was within 10%.

The local administered activity was compatible with the national DRL, although important margins for optimization were identified (up to a factor of 2) while still preserving RCmean and RCmax variations within

10%.

Conclusion

The support of medical physics, required by the law, resulted in optimized patient radiation protection while preserving image quality. The optimization process should be targeted to a particular clinical task and the collaboration between physicians, technologists and physicists is thus paramount.

Quantitative accuracy of Y-90-microspheres vial activities, results from PET experiments and Monte Carlo simulations

Silvano Gnesin[1]

[1]*Institute of Radiation Physics, Lausanne University Hospital, Lausanne*

Purpose

Y-90 radiolabelled resin and glass microspheres have been used for decades to treat primary hepatic carcinoma and liver metastases. Recently, experimental PET results [1] and Monte Carlo simulations [2] pointed out a possible important discrepancy between the calibrated activity and the actual activity present in both the Y-90 labelled resin and glass devices. The present communication aims to outline ad discuss the main results presented in the cited works and the possible clinical implications for the Y-90 radioembolization.

Methods

In [1], 56 glass and 18 resin's Y-90 labelled microspheres vials were measured in 5 PET/CT devices at four different institutions. The vial activity assessed by the PET (APET) was compared with the calibrated value reported by the manufacturer (AV). In [2], Monte Carlo simulations considering the actual glass/resin vial geometry and materials, the electric signal produced in a standard activity-meter configuration was estimated and compared between the two commercial products.

Results

Authors of [1] found the PET systematically underestimated (average -20%) / overestimated (on average +15%) the calibrated Y-90 activity in glass/resin vials. Accordingly, PET data showed an average difference of 46% between glass and resin microsphere activity calibrations. This experimental discrepancy was corroborated by the realistic Monte Carlo simulations reported in [2].

Conclusion

MC simulations performed in [2] indicate that the discrepancies recently found between PET/CT-measured activity and vendor-calibrated activity for Y-90 glass and resin microspheres [1] can be attributed to differences in the geometry of the respective commercial vials and to the metrologic approach adopted for activity meter calibration with a Y-90-chloride liquid source.

[1] Gnesin et al. J Nucl Med. 2022; https://doi.org/10.2967/jnumed.122.264458
[2] Auditore et al. J Nucl Med. 2023; https://doi.org/10.2967/jnumed.123.265494

Impact of reconstruction parameters in Luthetium-177 dosimetry

Milena Cristina Gravinatti[1], Andrea Zander[1], Hannes Grünig[1], Ujwal Bhure[1], Maria del Sol Perez Lago[1], Klaus Strobel[1], Thiago Lima[1]

[1]*Lucerne Cantonal Hospital, Lucerne*

Purpose

The aim of this work is to understand and characterise the impact of acquisition and reconstruction parameters in PSMA dosimetry.

Methods

A standardised phantom with known sphere sizes was used. Lesions and background were filled with 177Lu and the activity was set to mimic the ones found in patients. The phantom was then imaged in a clinical device with varying acquisition time (5, 10, 15 and 20 seconds per projection), matrix size (128x128 or 256x256), reconstruction iterations (5, 10, 15, 20, 25, 30, 35, 40, 45 and 50) and the use of post-processing Gaussian filter (0, 5 or 10mm). All other parameters were kept as per the manufacturer's recommendation (reconstruction method, subsets, angular trajectory, angular steps). The quantification was evaluated based on the sphere recovery coefficient for different sizes. The lung insert and the background were evaluated based on the residual lung error and coefficient of variance, respectively. Lastly, dosimetry based on the single time-point dosimetry implemented clinically was calculated for each generated dataset. Comparisons were made based on their spheres' absorbed doses both with respect to the mean values and dose volume histograms.

Results

The results demonstrated that acquisition statistics and reconstruction parameters significantly affected dosimetry measurements. Higher count statistics led to more accurate and precise dosimetry estimates, while shorter acquisition times led to higher variability in dose estimates. Negligible differences were observed for the evaluated voxel sizes. Standardization of acquisition and reconstruction protocols across different institutions may be necessary to ensure consistent dosimetry estimates and improve patient outcomes.

Conclusion

The findings of this study highlight the importance of SPECT acquisition and reconstruction parameters in PSMA dosimetry and their impact on accuracy and harmonization. The results suggest that acquisition statistics and reconstruction parameters should be carefully considered and optimized to improve the accuracy and consistency of dosimetry measurements.

Initial experience with dedicated eye lens dosimetry in interventional radiology

Davide Cester[1]

[1]*University Hospital Zurich and University of Zurich, Zurich*

Purpose

In 2020 our Institute introduced the use of dedicated eye lens dosimeters as an addition to the standard estimate through apron dosimeters. This work aims at providing a preliminary overview of our experience with the two methods used side-by-side.

Methods

The readings of the eye lens dosimeters have been compared to the official estimate calcolated from the under- and over-apron dosimeters, for three interventional radiologists over a period of around 60 man-months. The two most active radiologists performed on average similar procedures but worn different eye protection gear.

Results

The introduction of the additional dosimeter was in general well received and faced no insourmountable obstacles.

No clear correlation between the direct eye lens dose measurements and the estimated values could be observed.

The exposure recorded by the eye lens dosimeter was on average lower than the estimate by means of chest dosimeters, although the value ranges become similar when the most important correction factors are taken into account.

Conclusion

Dedicated eye lens dosimeters are an additional piece of equipment whose correct usage must be ensured in the daily routine.

The use of these additional dosimeters can simplify the evaluation of the eye lens exposure and reduce the associated errors, by removing variables with heavy influence like exposure geometry and effectiveness of the protecting gear.

Assessment of radiation dose values for fluoroscopy examinations in the operating theatre

Tristan Genetay[1], Axel Gamulin[1], Daniel Benamran[1], Laura Dupont[1], Lorimier Arnaud[1], Marta Sans Merce[1]

[1]Geneva University Hospital, Geneva

Purpose

Literature about radiation dose values following surgical examinations realised under X-ray fluoroscopy guidance is currently limited. Based on the recommendations of the International Commission on Radiological Protection, this study aims to provide reference dose levels in orthopaedic surgery, urology and vascular surgery at the University Hospital of Geneva.

Methods

A total of 2272 procedures were collected within 1 year using our Dose Archiving and Communication System (DACS). Exposure was defined in terms of dose-area product, fluoroscopy time and entrance air kerma at the reference point. For most common surgical procedures, median effective dose to patient were calculated using the Monte Carlo software PCXMC.

Results

The most irradiating procedures for each speciality were intramedullary nailing of proximal femur in orthopaedic surgery, percutaneous nephrolithotomy in urology and endovascular aortic aneurysm repair in vascular surgery. For these 3 procedures, the associated median DAP values/effective doses reported in this study were 1.17 Gy·cm^2/0.08 mSv, 14.95 Gy·cm^2/1.37 mSv and 27.23 Gy·cm^2/5.66 mSv respectively. According to FOPH ordinance on radiation protection, these 3 specialities can be classified into low dose, medium dose and high dose respectively. All values reported in this study were below the threshold for the deterministic effects of radiation.

Conclusion

The present study reported patient's exposure in common surgical procedures using fluoroscopy systems in the Geneva university hospital. Dose levels delivered to patients in vascular surgery and urology could be high and must become an object of concern for medical physicists. Patient's exposure in orthopaedic surgery were low, but optimisation is still possible to reduce further the dose while maintaining the image quality and limit stochastic effects in agreement with ALARA principle.

Microbeam radiation therapy: the next generation GRID-RT

Verdiana Trappetti[1], Liam Day[1], Valentin Djonov[1], Jennifer Fazzari[1], Cristian Fernandez-Palomo[1], Paolo Pellicioli[1], Cheuk Ting Wu[1]

[1]*University of Bern, Bern*

Purpose

Spatially fractionated radiotherapy (SFRT) is based on the principle of treating the total targeted volume with a non-uniform radiation dose in order to deliver much higher doses to portions of the malignancy. The oldest type of SFRT is known as GRID Radiotherapy (RT) and uses a perforated block positioned directly on the skin of the patient to partially screen the delivered homogenous beam of radiation. Our group at the university if Bern is working on the modern evolution of SFRT: microbeams radiation therapy (MRT). Our main purpose is to translate MRT to the clinic. To achieve our goal, in the last few years, we have extensively tested MRT in preclinical models to understand toxicity and treatment efficacy of this novel technique.

Methods

To generate MRT, we employed two 3rd generation Synchrotron facilities: the European Synchrotron Radiation Facility and the Australian Synchrotron. Synchrotron X-rays possess unique qualities including extremely high dose rates, a very small beam divergence, and a spectrum in the orthovoltage-energy range. These properties allow for the generation of microbeams with a very efficient dose deposition at the target site. Microbeam widths range in size from 25 μm to 100 μm, and the spacing between the microbeams ranges from 200 μm to 400 μm.

Results

Our research has demonstrated that MRT achieves excellent tumor control in several pre-clinical cancer models such as melanoma, lung carcinoma and glioblastoma. The remarkable dose-volume effect achieved by the MRT configuration, at ultra-high “FLASH” dose-rates of up to 12000 Gy/s, show minimal or no normal tissue radiation toxicity. We have demonstrated MRT sparing effects for various normal tissues including skin, lung, liver, and bone.

Conclusion

The preclinical work performed by our group paves the way to MRT clinical application for different types of malignancies.

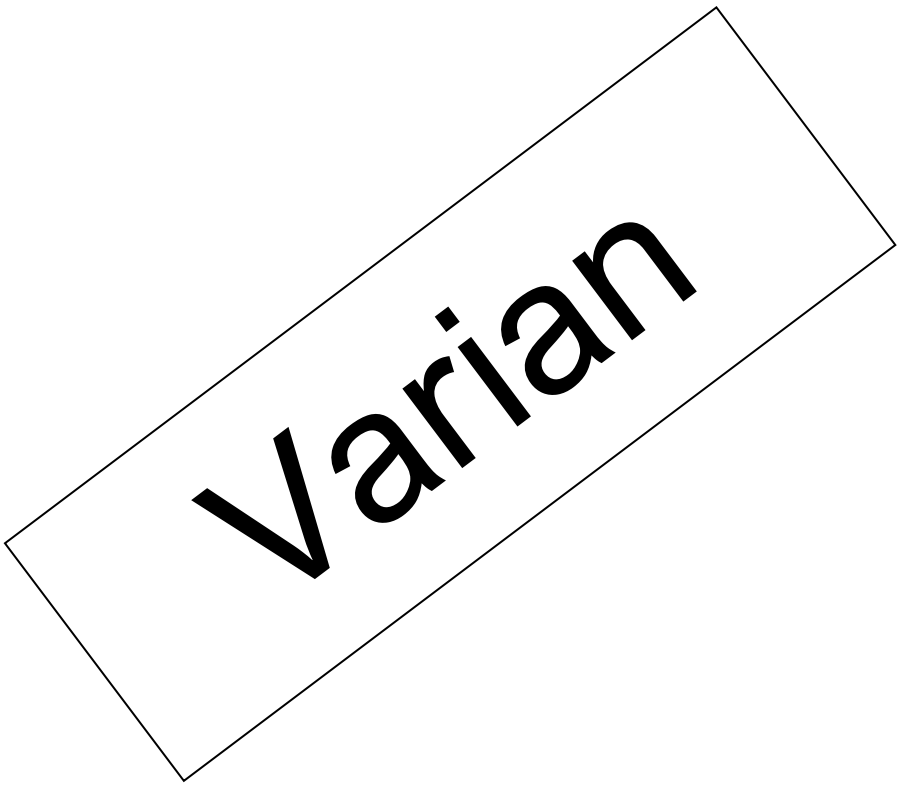
Varian

Modelling the biological effect of temporally feathered radiotherapy

Daniel Hosie[1,2], Jenny Bertholet[1], Michael Fix[1], Peter Manser[1], Marco F. M. Stampanoni[3]

[1]*Inselspital, Bern University Hospital and University of Bern, Bern*
[2]*Department of Physics, ETH Zurich, Zurich*
[3]*Department of Biomedical Engineering, ETH Zurich, Zurich*

Purpose

Temporally feathered radiotherapy (TFRT) replaces a standard treatment plan by 5 iso-curative sub-plans (López Alfonso et al. Med Phys 2018). Each sub-plan is created such that one of five chosen organs-at-risk (OARs) receives a higher dose compared to the standard plan in one fraction, allowing the other four OARs to receive a lower dose. Each OAR then receives one high and four low doses in alternation, weekly.

There are two potential benefits. First, TFRT can deliver a lower total physical dose to the feathered OARs by distributing the dose on different days. Second, a time-dependent normal tissue complication probability (NTCP) model suggests that the damage caused by the high dose is offset by increased repair during the low doses. However, the radiosensitivity parameters α, β, and recovery rate μ, needed for NTCP calculation are not well defined for OARs.

We investigate the potential benefit of TFRT for ranges of α, β, and μ, independently of the physical dose reduction effect.

Methods

We calculate OAR toxicity for a treatment delivering 2 Gy to the tumour in 25 fractions and a dose ds to the OAR in a standard fractionation. With TFRT, the high and low doses are ds + 0.4 Gy and ds – 0.1 Gy respectively so the total physical dose is the same as in the standard plan. Toxicity is calculated for ranges of α (0.05-1.00 1/Gy), μ (0.05-0.50 1/day) and ds (0.1-2.0 Gy), with β such that $\alpha/\beta = 3$ Gy (constant).

Results

The OAR toxicity reduction from TFRT for the investigated values is at the maximum $\alpha = 1.0$ 1/Gy, the minimum $\mu = 0.05$ 1/day and for ds = 0.3 Gy with a toxicity reduction of 11%-points. Of the investigated combinations, 14% reach a toxicity reduction of at least 1%-point and none have a negative effect for TFRT.

Conclusion

TFRT can reduce OAR toxicity compared to standard fractionation with the same total physical dose. However, radiobiological parameters must be determined.

Supported by Varian Medical Systems.

RT-EQD2: a tool for 3D evaluation of biologically weighted dose estimates

Lukas Wissmann[1], David Blumer[1]

[1]*Institute for Radiation Oncology, Spital Thurgau AG, Münsterlingen*

Purpose

Accurate and realistic dose accumulation in external beam radiotherapy planning becomes increasingly important in the context of repeat irradiations to returning patients. Rather than straight sums of physical dose, radiotherapy professionals prefer biologically weighted dose estimates to support prescription of repeat irradiations. This work presents a framework for creating biological dose estimate maps such as EQD2 for evaluation in a commercial radiotherapy treatment planning system (TPS).

Methods

A framework was programmed in Python 3.5 applying the linear-quadratic model to physical dose maps exported from the TPS (Varian Eclipse, Varian, Steinhausen, CH). Employed Python packages included pydicom, numpy, and DicomRTTool [1]. Dose maps were imported in Python using pydicom. Equivalent dose in fractions of 2 Gy (EQD2) maps were generated as follows: $EQD2 = n \cdot d \cdot (d+\alpha/\beta)/(d_2+\alpha/\beta)$, using point-wise array multiplication in numpy, where n = number of fractions, d = calculated dose per fraction, d_2 = 2 Gy and α/β is the alpha-beta ratio. EQD2 maps were generated with scalar α/β for the whole dataset, as well as in the form of arrays allowing spatially resolved α/β values. This enables application of organ-specific α/β in combination with contour masks extracted from RT-Struct files using DicomRTTool.

Results

EQD2 maps were computed and successfully imported into the TPS yielding EQD2 map overlays on the CT. Thereby, 3D-resolved display of biologically equivalent dose estimates are accessible in a clinical setting without the need for an external tool for visualization. Dose summation methods inside the TPS can be directly applied to evaluate the potential for repeat irradiations.

Conclusion

This work promotes a simple and slim solution for computation and display of 3D EQD2 maps inside the TPS. Direct applicability in clinical workflows fosters fast and accurate clinical decisions in interdisciplinary discussions about repeat irradiations. The framework may be extended to include further dose estimate models.

[1] Anderson, B.M. et al. Practical Radiation Oncology 2021, 11(3): 226-9

Revolutionizing particle therapy: a compact and cost-effective cyclotron-based proton facility

Vivek Maradia[1], Antony John Lomax[1], Damien Charles Weber[1]

[1]PSI – Paul Scherrer Institute, Villigen

Purpose

Particle therapy has shown clinical advantages over conventional radiation therapy, particularly for head and neck cancer and pediatric brain cancer treatment. However, limited availability is mainly due to high costs and facility size. Our goal is to design a more compact and cost-effective multi-room particle therapy facility using a cyclotron-based proton therapy approach.

Methods

Our method involves a rotating beamline without a gantry. The cyclotron is placed underground, and protons are guided to treatment rooms on the upper floor. Patients are treated in an upright position and rotated in front of a static treatment beam. The beamline can rotate 360 degrees in both directions. We used Monte Carlo simulations to calculate treatment beam characteristics.

Results

Our results show that a single-room proton facility can fit within an existing LINAC vault, and a 4-room facility can be housed within a tennis court area at a lower investment cost of around US$15-20 million. The rotating beamline design allows easy expansion to 12 treatment rooms without any major modifications. Monte Carlo simulations demonstrate that our beamline can transport full momentum spread, enabling broadened Bragg peaks and high dose rates for short field delivery times (5-10 sec), even for large tumors.

Conclusion

In conclusion, we have developed a compact, cost-effective, and high-performance beamline for a cyclotron-based proton therapy facility. This design could increase patient access to particle therapy, treating moving targets and accommodating various indications at a reduced cost compared to traditional radiation therapy.

First in-beam measurements of a multi-field proton treatment plan with the open-ring PETITION scanner

Keegan McNamara[1], Marina Béguin[2], Günther Dissertori[2], Judith Flock[2], Cristian Fuentes[2], Antony John Lomax[1], Shubhangi Makkar[1], Christian Ritzer[2], Damien Charles Weber[1], Carla Winterhalter[1]

[1]PSI – Paul Scherrer Institute, Villigen
[2]Physics Department, ETH Zurich, Zurich

Purpose

In-vivo range verification of proton therapy with PET provides a unique opportunity for 3D verification of treatment fields delivered to patients. In-beam and inter-field imaging is possible with use of an open-ring design, allowing uninterrupted delivery of treatment fields. We present the first proof of concept measurements for full in-beam and inter-field imaging using the recently designed open-ring PETITION PET scanner.

Methods

The current detector design is mountable in fixed imaging positions in Gantry 2 at PSI, whereas future clinical use would require manoeuvring between delivery of treatment fields, allowing seamless integration in clinic without loss of treatment quality. We simulate this possibility using a head phantom mounted to a rotatable jig. We deliver 3 treatment fields of 1 Gy RBE to a spherical target defined in the brain. The PET scanner acquires coincidences during the entire treatment period. Following delivery of each field the head phantom is rotated to a new position. The coincidences following each treatment field are then used to reconstruct images of the activity induced within the phantom.

Results

Reconstructed images following each field agree with the expected activity within 5mm in the distal fall off. We record coincidences for 15-20 minutes following each field, and record

total coincidences during each period. Between

(28-38%) of these counts occur in the first 2 minutes following each field. The rotation between delivery of each field significantly reduces the spatial distortion in the reconstructed images due to the opening. Measurement of the distal fall-off of multiple treatment fields allows for verification of CT predicted stopping power.

Conclusion

We have shown first measurements from the PETITION open-ring scanner for full treatment imaging of proton therapy. A rotatable design, either for gantry patients which rotates with the gantry to the next treatment position, or as a part of upright treatments with a fixed beam line and moving couch, provide imaging which may help reduce uncertainties in proton therapy.

A comprehensive analysis of RBE uncertainties and their potential clinical consequences for head and neck cancer

Lisa Stefanie Fankhauser[1], Carla Winterhalter[1], Nicola Bizzocchi[1], Carson Tully[1], Damien Charles Weber[1], Antony John Lomax[1]

[1]PSI – Paul Scherrer Institute, Villigen

Purpose

To evaluate the robustness of proton treatment plans to relative biological effectiveness (RBE) uncertainties based on target coverage and tissue toxicity using a normal tissue complication probability (NTCP) model.

Methods

Two different clinically used treatment planning techniques, a four-field and a six-field technique, combined with two optimization methods, planning target volume based and hybrid range robust, are assessed regarding their robustness to RBE uncertainties for four head and neck cancer cases. Two different RBE models, the McNamara and Wedenberg model, are combined with different tissue parameters and compared to the constant RBE model (RBE=1.1). Regarding assigning the tissue parameters, one can assign only to the GTV the tumour specific tissue parameter or to the whole CTV. In addition, there are different α/β ratios reported in multiple studies for the same tissue type. Two α/β ratios for healthy tissue (2Gy, 3Gy) combined with different ratios for the tumour tissue (8Gy,10Gy,12Gy) are investigated. The LET distribution and dose calculation are performed using Monte Carlo calculations (FRED GPU based).

Results

Overall, the investigated plans are sensitive to RBE uncertainties with deviations in NTCP values of up to +35% and -45% for the $V95$ endpoint. The Wedenberg model leads to a larger increase in NTCP values and a smaller decrease in target coverage compared with the McNamara model. Assigning α/β=12Gy compared to using α/β=8Gy for the target tissue leads to an additional target coverage loss of up to -30%. For the healthy tissue, using α/β=2Gy increases the NTCP value additionally up to +12% compared to α/β=3Gy. In addition, higher LET increases the RBE-weighted dose, hence, higher LET present in the tumour region can mitigate the effect of the high α/β ratio.

Conclusion

RBE uncertainties have been found to have a large impact on calculated NTCP and target coverage parameters. Therefore, it is important to consider the impact especially when comparing proton and photon treatment plans. Furthermore, using LET optimization could improve the robustness of the treatment plan to RBE uncertainties.

Comprehensive exploration of beam size and divergence variations in proton therapy facilities

Isabella Colizzi[1], Nicola Bizzocchi[1], Antony John Lomax[1], Vivek Maradia[1], David Meer[1], Serena Psoroulas[1], Damien Charles Weber[1]

[1]PSI – Paul Scherrer Institute, Villigen

Purpose

For a cyclotron-based facility, one of the methods for improving beam transmission is to transport higher emittance through the beamline, which can lead to larger beam sizes and/or divergence with respect to the ideal treatment planning requirements. A similar problem exists in multi-room facilities, where small differences between the transport beam lines for each treatment room can lead to different phase spaces in each room, complicating commissioning and quality assurance procedures. A comprehensive understanding of tolerance limits for beam size and divergence variations is also crucial for quality assurance procedures.

Methods

The investigation considers different scenarios involving the modification of beam size and divergence in the clinical PSI Gantry 2 beam model, either independently (keeping constant emittance) or together (modifying emittance). This covers a range of possible combinations that might be encountered during the commissioning of a new facility or beam optics scheme.

We optimized four plans on four major tumor types for proton therapy (CSI, Meningioma, Cranial Fossa, and Skull Base Chordoma) using the clinical beam model. We then recalculated the dose distributions, considering the different configurations of beam size and divergence, and evaluated their prescription fulfillment and plan quality in comparison to the optimized plan.

Results

Results indicate that, up to a beam size increase of 1.2 in the clinical PSI Gantry 2 beam model, dose distribution quality remains intact. Divergence adjustments exhibit considerable flexibility, with a factor change of 3 minimally impacting treatment quality. Emittance can be increased by up to 1.5 times solely by adjusting beam size or increased by up to 8-fold by modifying divergence without compromising plan quality.

Conclusion

In conclusion, variations in beam size exert a more substantial influence on dose distribution than changes in beam divergence. These findings have potential implications for setting commissioning and QA tolerance limits and simplifying the integration of new beam optics settings in existing facilities.

Direct aperture optimization-based pathfinding for non-isocentric dynamic trajectory radiotherapy applied to a craniospinal irradiation case

Gian Guyer[1], Jenny Bertholet[1], Silvan Müller[1], Kyriakos Rossis[1], Chengchen Zhu[1], Werner Volken[1], Daniel Aebersold[1], Peter Manser[1], Michael Fix[1]

[1]*Inselspital, Bern University Hospital and University of Bern, Bern*

Purpose

Non-isocentric dynamic trajectory radiotherapy (DTRT) is enabled through dynamic table translations in synchrony with intensity modulation and dynamic gantry, table and/or collimator rotation. Non-isocentric DTRT was shown to improve delivery time for craniospinal irradiation (CSI) compared to multi-isocentric intensity modulated radiotherapy (IMRT) by moving the table longitudinally during beam-on. However, a manual plan setup for non-isocentric DTRT is time-consuming and challenging, due to the multiple dynamic axes. We aim to develop a pathfinding strategy for non-isocentric DTRT based on a direct aperture optimization (DAO) for a CSI case.

Methods

The DAO-based pathfinding considers all available beam directions, given by a gantry angle and longitudinal table position grid with 10° and 8 cm resolution, respectively. Promising beam directions are iteratively added until a user-chosen total path-length is reached, resulting in a gantry-table path. In each iteration, the available beam directions are restricted such that every direction can only be added once and no reverse motion of gantry or table is allowed. DAO determining the intensity modulation along the generated gantry-table path, resampled to a spacing of 5° (gantry) and 2 cm (table), generates final plans. Two non-isocentric DTRT plans are created and compared for one CSI case: one with a manual path setup and one with the DAO-based pathfinding strategy. The manual path setup consists of a longitudinal table translation along the spinal cord, a gantry rotation around the head and a longitudinal table translation back along the spinal cord.

Results

DAO-based pathfinding generates a similar path to the manual setup with maximum deviation of 40° in gantry angle from the manual path. Target coverage and homogeneity are similar in both plans with equivalent dose to organs-at-risk. The estimated delivery times are 2.8 min (DAO-based pathfinding) and 2.9 min (manual path setup).

Conclusion

We successfully developed a DAO-based dosimetrically motivated pathfinding strategy applied to a CSI case, promising a more automated treatment planning process for non-isocentric DTRT.

Disclosures

Supported by grant 200021_185366 of the SNSF and Varian Medical Systems.

Comparison of geometric and dosimetric-based path-finding for dynamic collimator-radiotherapy (colli-DTRT)

Annalisa Walpen[1], Chengchen Zhu[1], Jenny Bertholet[1], Gian Guyer[1], Hannes A. Loebner[1], Silvan Müller[1], Marco F. M. Stampanoni[2,3], Michael K. Fix[1], Peter Manser[1]

[1]Inselspital, Bern University Hospital and University of Bern, Bern
[2]PSI – Paul Scherrer Institute, Villigen
[3]Department of Biomedical Engineering, ETH Zurich, Zurich

Purpose

Dynamic-collimator trajectory radiotherapy (colli-DTRT) delivers intensity modulated radiotherapy with non-coplanar partial arcs and dynamic-collimator rotation. We compare two path-finding approaches for colli-DTRT, geometric and dosimetric, investigating the impact of organ-at-risk (OAR) prioritization on the path-finding and dosimetric plan quality.

Methods

In the geometric path-finding approach, paths are determined on a gantry-table-map quantifying the fractional target/OAR overlap (cost) for possible beam directions based on path-cost and gantry-angle-range. The dosimetric approach determines paths via iterative fluence-map-optimization (FMO) and beam elimination, rejecting the lowest contributing fields to the mean PTV dose. For both approaches, colli-DTRT plans are generated by determining the intensity modulation along the resulting paths using a direct-aperture optimization followed by a final dose calculation. OAR prioritization can be performed by increasing the weight of the OAR-specific gantry-table-map (geometric approach) or the dose objective priority (dosimetric approach). For an adenoid cystic carcinoma case (elective target volume, 25 x 2 Gy), we focused on sparing the ipsilateral submandibular gland (ISMG) located in proximity to the target. colli-DTRT plans were generated for weights 2-10 and for objective priorities scaled by a factor 2-10 and compared to a reference plan (RP) with uniform weight of 1 (geometric-RP) or uniform objective priorities (dosimetric-RP) for all OARs.

Results

Similar target coverage was achieved for all plans. Improved sparing of the ISMG was observed with increasing objective priority for the dosimetric approach, while an increased weight in the geometric approach did not always translate into a better sparing. For the geometric approach, the highest sparing of ISMG was achieved with weight 8, reducing Dmean by 0.3 Gy compared to geometric-RP. Dosimetric colli-DTRT plans reduced Dmean to ISMG by 0.3-0.9 Gy compared to dosimetric-RP and by 2.3-2.9 Gy compared to geometric-RP.

Conclusion

Prioritization of OARs is possible at the path-finding stage for both geometric and dosimetric approaches. Consideration of dosimetric instead of geometric information in the path-finding process leads to superior OAR sparing for the investigated case.

Disclosures

Supported by SNSF grant 200021_185366 and Varian Medical Systems.

Robust dynamic-collimator trajectory radiotherapy (colli-DTRT)

Alina Paunoiu[1,2], Jenny Bertholet[1], Gian Guyer[1], Hannes A. Loebner[1], Chengchen Zhu[1], Silvan Mueller[1], Marco F. M. Stampanoni[2,3], Peter Manser[1], Michael Fix[1]

[1]Inselspital, Bern University Hospital and University of Bern, Bern
[2]Department of Biomedical Engineering, ETH Zurich, Zurich
[3]PSI – Paul Scherrer Institute, Villigen

Purpose

To develop robust dynamic-collimator trajectory radiotherapy (colli-DTRT), including robust dosimetrically motivated path-finding, to manage patient set-up uncertainties.

Methods

colli-DTRT plans were created for one brain (30 x 2 Gy) and one breast (16 x 2.65 Gy) clinically motivated cases. colli-DTRT paths were generated through iterative fluence map optimization (FMO) and beam angle elimination. Direct aperture optimization (DAO) was applied to the paths to obtain a deliverable plan. Standard planning target volume (PTV) plans (colli-DTRT

) were optimized using a PTV extending the clinical target volume (CTV) by 3 mm (brain) and 5 mm (breast). Robust plans (colli-DTRT

) were optimized directly on the CTV using robust FMO during path-finding and robust DAO for final plan optimization considering 5 mm systematic shifts in all three directions. All plans were normalized to 50% of the PTV/CTV. Plan quality and robustness were evaluated by comparing dose-volume endpoints of the nominal scenario and the standard deviation (σ) of the mean over all scenarios.

Results

For the brain case, $D_{98\%}$ to the CTV was 58.0 Gy (σ = 1.1 Gy) for colli-$DTRT_{PTV}$ and 57.3 Gy (σ = 2.2 Gy) for colli-$DTRT_{robust}$. $D_{2\%}$ to the right optic nerve was 38.1 Gy (σ = 10.5 Gy) for colli-$DTRT_{PTV}$ and 32.5 Gy (σ = 6.0 Gy) for colli-$DTRT_{robust}$. For the breast case, $D_{98\%}$ to the CTV was 41.0 Gy (σ = 0.3 Gy) for colli-$DTRT_{PTV}$ and 40.6 Gy (σ = 0.3 Gy) for colli-$DTRT_{robust}$. D_{mean} to the right lung was 12.2 Gy (σ = 0.9 Gy) for colli-$DTRT_{PTV}$ and 11.8 Gy (σ = 0.8 Gy) for colli-$DTRT_{robust}$.

.

Conclusion

Robust colli-DTRT with robust dosimetrically motivated path-finding was successfully developed, improving organs at risk sparing and robustness compared to the PTV approach for two investigated cases. However, target coverage was higher in colli-$DTRT_{PTV}$ than colli-$DTRT_{robust}$ for both cases. Robustness of target coverage was the same for the breast case but better with colli-$DTRT_{PTV}$ than colli-$DTRT_{robust}$ for the brain case.

Disclosures

Supported by SNSF grant 200021_185366 and Varian Medical Systems.


medisynt /
Solumedics

JulianA: automatic spot weight optimisation for proton radiotherapy

Renato Bellotti[1], Alexey Cherchik[1], Jonas Willmann[1], Damien Charles Weber[1], Antony John Lomax[1], Andreas Adelmann[1], Jan Hrbacek[1]

[1]PSI – Paul Scherrer Institute, Villigen

Purpose

To introduce JulianA, a novel algorithm for automatic treatment planning for proton therapy (PT). Its name combines our in-house treatment planning system, FIonA, with the Julia programming language.

Methods

JulianA utilises a novel plan quality scoring system tailored to represent the clinical intent, encompassing prescribed dose levels and organ-at-risk (OAR) dose constraints. The algorithm requires only target levels and OAR threshold values as input. By optimizing this plan score, JulianA generates the final dose distribution. Validation was conducted through a retrospective planning study comprising six head-and-neck cases treated with PT using a simultaneous integrated boost delivery paradigm with prescribed dose levels 54.12 Gy, 59.4 Gy and 69.96 Gy at the Center for Proton Therapy. All parameters were derived from two patients within this dataset, eliminating the need for additional training data.

Results

Automatically generated JulianA plans exhibited comparable quality to human-made reference plans. Target V95% differences between reference and JulianA plans were within a narrow range: -0.1% ± 1.5%, 0.1% ± 2.2%, and 1.2% ± 2.7% (mean ± standard deviation) for low, medium, and high-dose targets, respectively. JulianA consistently reduced maximum doses to the brainstem center, brainstem surface, chiasm, and retinae, as well as mean doses to the lacrimal glands in all patients. However, some OARs showed increased maximum or mean doses in at least one patient. JulianA's worst performing endpoints were observed for mean dose to the right cochlea (increase of 0.6 ± 2 Gy) and maximum dose to the right temporal lobe (increase of 0.1 ± 2.7 Gy). The algorithm exhibited efficient planning times, with an average of 15.6 ± 5 minutes (maximum 23.3 minutes).

Conclusion

Preliminary findings demonstrate that JulianA is capable of automatically generating head-and-neck treatment plans for PT comparable in quality to those created by human experts. Ongoing validation efforts, including assessment by radiation oncologists, aim to further evaluate JulianA's potential in a clinical setting.

Impact of penumbra sharpness on lateral margin requirement for ocular proton therapy

Daniel Björkman[1], Riccardo Via[1], Maria De Prado Leal[1], Antony John Lomax[1], Guido Baroni[2], Damien Charles Weber[1], Jan Hrbacek[1]

[1]PSI – Paul Scherrer Institute, Villigen
[2]Politecnico Di Milano, Milan

Purpose

Ocular malignancies are treated worldwide with proton therapy using a diverse set of accelerator delivery systems. Lateral margin usage remains consistent, despite variations in dose characteristics. This study quantifies the interchangeability of lateral margin and penumbra sharpness in ocular proton therapy, addressing a key treatment optimization factor.

Methods

In this study, we investigate permissible offsets to the intended clinical eye orientation by assessing resulting target coverage for a cohort of 16 patients. Using a point cloud model of the eye, we applied translations and measured translation-induced rotations to identify the three-dimensional boundary conditions which ensures adequate target coverage. We explored a range of lateral margins and dose penumbras, as reported from different operational treatment facilities around the world.

Results

Our investigation defines a range of offsets for the investigated cohort within which target coverage is preserved for the investigated lateral margins and penumbras. Initial findings utilizing the dose field characteristics of the Optis treatment room at Paul Scherrer Institut in Switzerland, indicate that target coverage for all patients would remain uncompromised even for deviations within 0.5 mm, 0.5 mm, and 1.5 mm along the x, y, and z axes of the treatment room. In contrast, the cohort-wide median representation showed values of 1.0, 1.0, and 2.8 in the x, y, and z dimensions, respectively. The findings indicate that the comparable offset tolerance for a given treatment facility can be calculated using the equation: Lateral margin = $1.6 * x + 0.9$, where x represents the ratio of representative penumbra sharpness of the facility over that of Optis.

Conclusion

Our results establish a benchmark for selecting appropriate lateral margins based on the dose characteristics specific to the treatment facility, ensuring equivalent robustness between facilities to errors in patient positioning and intra-fractional motion.

Tissue assignment using combined MR CT for activation calculations in pencil beam scanning proton therapy patients

Anne zur Horst[1], Keegan McNamara[2], Marina Béguin[1], Günther Dissertori[1], Judith Flock[1], Cristian Fuentes[1], Antony John Lomax[2], Shubhangi Makkar[2], Christian Ritzer[1], Damien Charles Weber[2], Carla Winterhalter[2]

[1]Physics Department, ETH Zurich, Zurich
[2]PSI – Paul Scherrer Institute, Villigen

Purpose

To improve the prediction of positron emission tomography (PET) activity for treatment verification of proton therapy, magnetic resonance (MR) and computed tomography (CT) images were combined to assign an elemental composition to voxels within the CT based on the tissues identified in the MR.

Methods

Clinical treatment plans were generated for six head and neck patients. The diagnostic MR image was registered to the planning CT image, segmented and the elemental composition was masked based on grey/white matter, cerebrospinal fluid, or tumour. PET simulations were performed both with calibration of elemental composition based on the Schneider method for converting Hounsfield units to material information and using a MR-based calibration. Monte Carlo methods were used to score the most abundant radioactive isotopes. The coincidence signal detection of a full-ring PET scanner was simulated and image reconstruction was performed. Most Likely Shift (MLS), Middle Point (MP), and an iso-activity analysis were used to analyse the distal end of profiles along the field axis.

Results

For the selected timeframes, approximately 80% of the total activation was due to O-15, with its distribution depending on oxygen content of irradiated tissues. MR-based distributions were less noisy compared to those using CT-calibration. Iso-activity analysis showed distance-to-agreements (DTA) of up to several centimetres in extended regions of tissue re-assignment and shifts of ±3 mm in MLS. Setup errors could be detected with MLS and MP, with MLS being more robust to changes in calibration. The reconstructed images however were noisy for simulated measurement timeframes of 30 seconds. Standard deviations of detected shifts ranged from 3 to 5 mm. For both MLS and MP, the DTA in iso-activity levels was mostly within ±5 mm.

Conclusion

The determination of the oxygen content of irradiated tissues is essential for reliable PET activation calculations, influencing range evaluation methods. The inherent uncertainty introduced with image acquisition and reconstruction however limits the ability to identify small differences.

Improving proton therapy delivery efficiency via combination of advanced spot positioning algorithms and ridge filter

Martina Bonomi[1], Nicola Bizzocchi[1], Isabella Colizzi[1], Antony John Lomax[1], Vivek Maradia[1], David Meer[1], Serena Psoroulas[1], Damien Charles Weber[1]

[1]PSI – Paul Scherrer Institute, Villigen

Purpose

Rescanning, gating, and breath-hold are promising approaches for realising proton therapy treatments of moving targets, but decrease delivery efficiency, lengthening treatment delivery time. In PBS (Pencil Beam Scanning) proton therapy, two factors influence the treatment delivery time: the beam-on time and the dead time, which is the time required for energy-layer and spot-position adjustments. Several studies demonstrated that ridge filters (RFs) effectively decrease the dead time by reducing the number of energy layers and therefore of spots. Further, the use of different spot placement techniques can reduce dead time by minimizing the number of spots required. However, clinics use different spot placements, with no consensus on the optimal one, and RFs are not employed clinically in PBS proton therapy. In this study, we examined the advantages and limitations of combining a RF with various spot placement techniques to reduce the delivery time without compromising the plan quality, to pave the way for a future clinical implementation.

Methods

We created treatment plans on a cohort of 12 different patients affected by lung tumors assuming a RF that broadens the Bragg peak into a Gaussian shape, in combination with a fixed grid-based spot placement technique (FG configuration), an energy-dependent technique based on the beam's size in air (A configuration) and in water (W configuration). These configurations were compared in terms of plan quality and clinical acceptability.

Results

Results indicated that FG plans showed the best performance. The A and W plans, instead, performed poorly, with W plans providing the worst results and not yielding any acceptable plans due to the treatment planning system being constrained by a limited number of degrees of freedom.

Conclusion

In conclusion, by combining RF-broadened Bragg peaks with a spot placement algorithm based on a fixed grid, we can obtain treatment plans with good clinical quality and significantly reduce delivery time, improving the overall quality of the treatment, and thus potentially increasing 4D treatment feasibility.

Synchrony modality on Radixact: evaluation of the targeting accuracy

Marie Fargier-Voiron[1], Anthony Nagy[1], Nicolas Perichon[1], Cédric De Marco[1], Mireille Conrad[1], Oscar Matzinger[1], Maud Jaccard[1]

[1]Clinique de Genolier and Clinique Générale-Beaulieu, Swiss Radio-Oncology Network, Genolier

Purpose

The Radixact Synchrony modality enables to correct in real-time for tumor motion during tomohelical treatments by adjusting jaws and/or MLC position (Schnarr, 2018). The Synchrony precision was already investigated but only with gamma index methodology, which prevents discrimination between dose and geometric errors. Thus, the aim of this study is to quantify the Synchrony targeting accuracy by adapting the Cyberknife End-To-End (E2E) methodology on the Radixact machine.

Methods

All available tracking methods were evaluated: fiducial (FID), fiducial with respiratory motion (FIDResp), and lung with respiratory motion (LResp). Plans were generated with RayStation12A on anthropomorphic phantoms that allow the insertion of two perpendicular radiochromic films centered on a sphere representing the target. The prescription dose of 4.2 Gy was set to the 70% isodose around the target. Calculated dose distributions were strictly identical between plans without and with Synchrony.

The reference targeting accuracy was first determined (Synchrony off, no motion). Then different scenarios were compared to the reference one, from the simplest (Synchrony on, no target motion) to the most complex (Synchrony on, multiple simultaneous target motions in different directions). The targeting accuracy was determined by calculating the difference on each direction between the dose distribution center and the geometric center of the films. The total targeting error (TTE) was determined using the Accuray's E2E software.

Results

TTE values were <1 mm for the reference scenario for each tracking method (FID: 0.3 mm; FIDResp: 0.5 mm; LResp: 0.8 mm). With the simple activation of the Synchrony and no motion, TTE exceeded 1 mm, with a systematic 0.7 mm longitudinal discrepancy. With more complex scenario including motion during delivery, applying MLC corrections led to TTE >2 mm.

Conclusion

The E2E methodology developed in this study revealed a systematic discrepancy of 0.7 mm in the longitudinal direction when using the Radixact Synchrony modality, leading to large values of TTE inadequate for stereotactic treatments. This error is currently being investigated by the company with a view to proposing a short-term corrective solution.

Robust optimization of lung SBRT treatments using CyberKnife with Synchrony and X-Sight Spine tracking methods

Maude Gondré[1], François Bochud[1], Jean Bourhis[2], Raphael Moeckli[1], Véronique Vallet[1]

[1]*Institute of Radiation Physics, Lausanne University Hospital, Lausanne*
[2]*CHUV – Centre Hospitalier Universitaire Vaudois, Lausanne*

Purpose

To assess the dosimetric gain on ipsilateral lung using robust optimization on the GTV (GTV-based) or ITV (ITV-based) instead of standard PTV optimization (PTV-based) for lung stereotactic body radiotherapy (SBRT) on the CyberKnife with Synchrony and X-sight spine tracking methods.

Methods

For on-line synchrony tracking, 15 lung SBRT were calculated with both GTV- and PTV-based methods. The GTV-based plans were optimized using a robust margin corresponding to the GTV-PTV margin. For x-sight spine static tracking, 5 lung SBRT were calculated with GTV-, ITV- and PTV-based methods. Both GTV-and ITV- based plans were optimized with a robust margin corresponding to the ITV-PTV margin. For GTV-based plans, all phases of the 4D-CT were included in the optimization. For all plans, a robust evaluation was performed to assess dose to ipsilateral lung, as well as the GTV coverage for all treatment scenarios (combination of positional uncertainty and respiratory motion). Dose to the ipsilateral lung (Dmean, V20Gy and V5Gy) as well as the GTV coverage were recorded.

Results

For synchrony tracking, the average Dmean of the ipsilateral lung was reduced by 0.7 Gy with GTV-based method. The V5Gy was reduced from 22.31% for PTV-based to 18.02% for GTV-based plans. The V20Gy was reduced from 4.45% for PTV-based to 3.24% for GTV-based plans. The coverage of the GTV was fulfilled for all scenarios for both GTV- and PTV-based plans. For x-sight spine tracking, the average Dmean was reduced by 0.95 Gy for ITV- and by 1.03 Gy for GTV-based plans compared to PTV-based plans. The V20Gy was reduced from 9.17% for PTV-based plans to 7.42% and 7.25% for ITV- and GTV-based plans respectively. The V5Gy was reduced from 31.77% for PTV-based plans to 28.45% and 28.41% for ITV- and GTV-based plans respectively. The GTV coverage was in the tolerance for all scenarios.

Conclusion

Robust optimization, considering the positional uncertainty and the respiratory motion during optimization, allowed to reduce dose to ipsilateral lung while maintaining an adequate GTV coverage.

Reference dosimetry for electron FLASH radiotherapy at METAS

Peter Peier[1], Franziska Frei[1]

[1]*METAS, Bern*

Purpose

Radiotherapy with ultra-high dose rates (UHDR) or FLASH radiotherapy (RT), offers the potential of significant reduction in side effects for cancer patients, and associated improvement in quality of life. In the short term, new electron and proton beam facilities for FLASH are currently being installed or being upgraded to FLASH mode. The clinical application of such radiation requires precise and traceable dose measurement. The dose measuring devices used in conventional radiotherapy are only suitable for this to a very limited extent.

Methods

METAS as part of a strong international consortium took part in the development of a metrological framework for UHDR beams within the European project UHDpulse. Primary as well as secondary standards for absorbed dose-to-water measurements were tested for their suitability in UHDR beams.

METAS established an UHDR reference electron beam. It improved its primary standard for UHDR electron beams and investigated the behaviour of well-known and new detectors in such beams.

Results

METAS modified its accelerator to provide electron pulses with up to 1Gy/pulse in 3μs at 15MeV beam energy.

A comparison of the Fricke primary standard with the PTB water calorimeter showed excellent agreement. The ratio between the dose delivered by a calibrated UHDR electron beam using the METAS primary standard and the dose delivered by a calibrated UHDR electron beam using the PTB primary standard was shown to be 1.002(12).

METAS, investigated several detector types, such as parallel plate ionization chambers, diamond detector, Fricke dosimeter, EBT3 film and Alanine. The widespread parallel-plate ionization chambers showed strong electron recombination effects in UHDR beams that distort the dose measurement significantly. Hence, the common correction models cannot be used. The passive detectors, on the other hand, did not show a dose rate-dependent response.

Conclusion

It has been shown that conventional detectors (mainly ionisation chambers) are not readily usable for reference dosimetry in UHDR beams. Therefore, METAS established reference dosimetry for UHDR electron beams which will be presented in this contribution.

Influence of age and breast density on the radiation dose received for a mammography examination

Laura Dupont[1], Marta Sans Merce[1]

[1]*HUG - Hôpitaux Universitaires de Genève, Geneva*

Purpose

The breast is a radiation-sensitive organ, and its composition varies from one individual to another. But does its composition affect the dose received during a mammography examination? The objective of this study is to determine the influence of age and breast density on the dose of radiation received during a mammography examination.

Methods

A retrospective study was conducted using all Digital Breast Tomosynthesis (DBT) examinations performed in 2020 and 2021 with the Selenia Dimension mammography unit by Hologic at the University Hospitals of Geneva (HUG). Seven categories of compressed breast thickness (CBT) were defined, with 10 mm intervals ranging from 20 mm to 90 mm. Data analysis was carried out for each thickness category, considering age, breast density, mean glandular dose (MGD), and entrance dose (ED). Three relationships were studied across the seven CBT categories: the change in breast density with age, the influence of breast density on the received dose, and how the dose received varies with age.

Results

Out of 1622 mammography acquisitions subjected to analysis, 1205 met the study's eligibility criteria, involving patients aged 28 to 100 years, with an average age of 58 years, and with varying breast densities classified from A to D.

We examined the correlations among age, density, and the received dose for the seven CBT categories.

The analysis showed that breast density declines as age advances, and that the dose rises as the breast density increases, within all the thickness categories.

As an implication of the preceding findings, the dose exhibited a decrease as age increased, regardless of breast thickness.

These results highlight how breast density, which varies with age, affects the dose received during mammography examinations.

Conclusion

These findings substantiate a correlation between breast density and age, as well as a correlation between breast density and administered radiation dose, and between age and radiation dose. These findings could be an important asset to take into account when establishing Diagnostic Reference Levels (DRLs) for mammography.

Optimization of CT pulmonary angiography using task-based image quality assessment and diagnostic reference levels: An example of the implication of medical physicists in CT

Anais Viry[1], Veronika Vitzthum[1], Pascal Monnin[1], Marie Nowak[1], Julie Bize[1], David Rotzinger[1], Damien Racine[1]

[1]CHUV – Centre Hospitalier Universitaire Vaudois, Lausanne

Purpose

In accordance with Article 36 of the Radiation Protection Ordinance (ORap), medical physicists must be involved in all CT applications, particularly for the optimization of CT protocols. In this framework, the purpose of this study is to establish size specific diagnostic reference levels (DRLs) for pulmonary embolism (PE) based on patient CT examinations performed on 74 CT devices in the French part of Switzerland. Then, to assess task-based image quality (IQ) for each device and to investigate the variability of dose and IQ across different CTs. Finally, to propose a dose-IQ optimization for each CT.

Methods

1051 CT pulmonary angiography dose data were collected for one year. Two categories of patient sizes (medium and large) were established from the distribution of the thoracic perimeters. DRLs were calculated as the 75th percentile of volumetric CT dose index (CTDIvol). IQ was assessed with two thoracic phantom sizes using local acquisition parameters and three other dose levels. The area under the ROC curve (AUC) of a 2mm low-perfused vessel was assessed with a non-prewhitening with eye-filter model observer. The optimal IQ-dose relationship was mathematically assessed from the fitted curve between IQ and dose. The variability across different CTs before end after applying the proposed optimization were described using the interquartile of dose and AUC values.

Results

The DRLs of CTDIvol were 6.4mGy and 10mGy for the two patient sizes. 75th percentile of phantom CTDIvol were 6.3mGy and 10mGy for the two phantom sizes with inter-quartile AUC values of 0.047 and 0.066, respectively. After optimization, phantom CTDIvol decreased to 5.9mGy and 7.5mGy and the interquartile AUC values were reduced to 0.025 and 0.057 for the two phantom sizes, respectively.

Conclusion

DRLs for pulmonary embolism were proposed as a function of patient thoracic perimeters. The agreement between patient and phantom doses were shown. This study highlights the variability in terms of dose and IQ. The implication of medical physicists in CT to optimize protocols can lead to a global harmonization of dose and IQ.

Integrating temporal resolution on the non-prewhitening model observer in computed tomography

Damien Racine[1], Pascal Monnin[1], Marie Nowak[1], David Rotzinger[1], Anais Viry[1], Veronika Vitzthum[1]

[1]*CHUV – Centre Hospitalier Universitaire Vaudois, Lausanne*

Purpose

Image quality in computed tomography is generally assessed using model observers (MO) without integrating the influence of temporal resolution. The aim of this study was to develop a methodology to integrate the temporal resolution in MO.

Methods

A cubic water phantom containing a cylinder in polymethyl methacrylate was scanned using various acquisition parameters (rotation times, pitch factors and collimation widths) on two CT systems, a wide-detector and a dual-source. The phantom was firstly scanned without a motion to determine the in-plane task-based transfer functions (TTF) and noise power spectra (NPS). Then, it was scanned on a moving platform with a uniform rectilinear motion in the transverse plane tocalculate the temporal modulation transfer function (MTFt). The longitudinal TTF was measured using a thin tungsten wire. At the end, the metrics were introduced in a specific spatiotemporal formulation of the non-prewhitening with eye filter MO to assess the detectability (d') of moving objects with a speed of 20 $mm \cdot s^{-1}$.

Results

Varying rotation time, helical pitch, collimation width had minimal impact on in plane and longitudinal spatial resolution and noise. MTFt showed that increasing tube rotation time, collimation width, and pitch factor improved the temporal resolution.

In comparison to d' calculated without movement, on the dual-source CT, d' decreased by 23.5%, 43.1% and 56.9% for the rotation times 0.25, 0.50 and 1.0 s, respectively. On the wide-detector CT, d' decreased only by 14.0% for the minimal rotation time of 0.23 s, and by 51.2% for the maximal rotation time of 1.0 s. On the dual-source system, d' decreased by 50.6% for the smallest pitch and by 9.5% for the largest pitch. On the wide-detector system, d' decreased by 40.4%, 18.8%, 7.6% and 4.9% for the pitch 0.516, 0.984, 1.375 and 1.531, respectively.

Conclusion

Faster rotation time, higher pitch factors, and larger collimation widths improved temporal resolution without compromising in-plane and longitudinal resolution or noise. However, caution should be exercised regarding over ranging when using large pitch factors and large collimations.

Patient eye lens radiation exposure during interventional neuroradiology procedures

Elina Samara[1], Stephanie Tanadini-Lang[1], Anja Stüssi[1], Zsolt Kulcsar[1], Matthias Guckenberger[1]

[1]*University Hospital Zurich and University of Zurich, Zurich*

Purpose

Neuroradiological interventions are minimally invasive procedures that can provide diagnostic information and offer treatment for diseases such as an ischemic stroke or cerebral aneurysm. These procedures have several advantages for the patient, such as fewer complications than open operations and shorter recovery times. However, they are accompanied by radiation exposure. Aim of this study was to determine which type of neuro-interventional procedures are associated with high eye-lens exposure for patients and the factors that affect the eye-lens exposure.

Methods

Real-time measurements were performed on thirty-six patients who underwent diagnostic or therapeutic neurointerventional procedures. Gafchromic™ XR-RV3 films were placed for radiation dose measurements near patients' eyes. The films were calibrated against an orthovoltage X-ray device (Gulmay Medical) and read with a dedicated scanner.

Results

The dose-area product, fluoroscopy time and cumulative air-kerma were collected for every patient. The median eye dose during neurointerventional procedures was 150 mGy, as measured with the Gafchromic films, with a maximum of 1007 mGy in a single procedure. The mean dose for the left eye (located toward the lateral C-arm X-ray source) was 1.5 times higher than the mean dose for the right one. Doses to the left eye showed better correlation with the air-kerma (r^2=0.7) for diagnostics procedures than for therapeutic (r^2=0.4), probably because of the complexity of the latter (primary beam, multiple beam projection, etc.).

Conclusion

Some patients may receive eye doses exceeding the threshold of tissue reaction, especially on the left side. High eye dose are mainly related to therapeutic procedures. A careful optimization of the procedures and follow-up of these patients to evaluate potential lens opacities should be considered.

Probabilistic U-Net model observer for the DDC method in CT scan protocol optimization

David Stocker[1], Christian Sommer[1], Sarah Gueng[1], Jason Stäuble[1], Ismail Özden[2], Jennifer Griessinger[1], Matthias Weyland[1], Gerd Lutters[2], Stephan Scheidegger[1]

[1]ZHAW - Zürcher Hochschule für Angewandte Wissenschaften, Zurich
[2]Kantonsspital Aarau, Fachstelle Strahlenschutz und Medizinphysik, Aarau

Purpose

The task of co-optimizing dose and image quality is challenged by technological advancements in Computed Tomography (CT), including Machine Learning (ML)-driven image reconstructions. Conventional methods of image quality assessment often fail to capture radiologists' clinical perspective. To address this, a method based on the Difference-Detailed Curve (DDC) has been developed, involving human observers assessing low-contrast object visibility in purpose-designed phantoms. Due to the labor-intensive and variable nature of this procedure, automating and standardizing with ML models emulating human observers is desirable.

Methods

A Bayesian model observer framework is formulated to generate well-calibrated probabilistic low-contrast object visibility predictions, which plays a crucial role in quantifying observer variability. Additionally, a reliability indicator for probability predictions is introduced by estimating an "effective number of observations". This quantifies the extent to which the trained model observer effectively utilizes observations in the training set for predictions on the test set. Using this framework, a 3D U-Net model observer is trained on a dataset containing 15 phantom scans, each featuring 60 imaged low-contrast objects assessed by 10 observers. The model's performance is subsequently evaluated on 9 additional scans.

Results

Accurate visibility probability predictions are achieved on the test set, demonstrating a Mean Squared Error of 0.011 and an estimated effective number of observations of 8.3, indicating that statistically, the trained model observer incorporates information from approx. 8 human observers. Most importantly, these predictions yield a distribution of DDCs that closely mirrors the DDCs observed by human observers on the test dataset.

Conclusion

The introduction of the Bayesian framework enables the selection of a standardized model observer tailored to the task at hand by choosing an appropriate probability threshold. Moreover, notable practical results have been attained even with a limited training dataset of only 15 scans. However, it is crucial to emphasize that while the obtained results are promising, ensuring the reliability and generalizability of the probabilistic model observer and its methodology demands validation on a larger dataset.

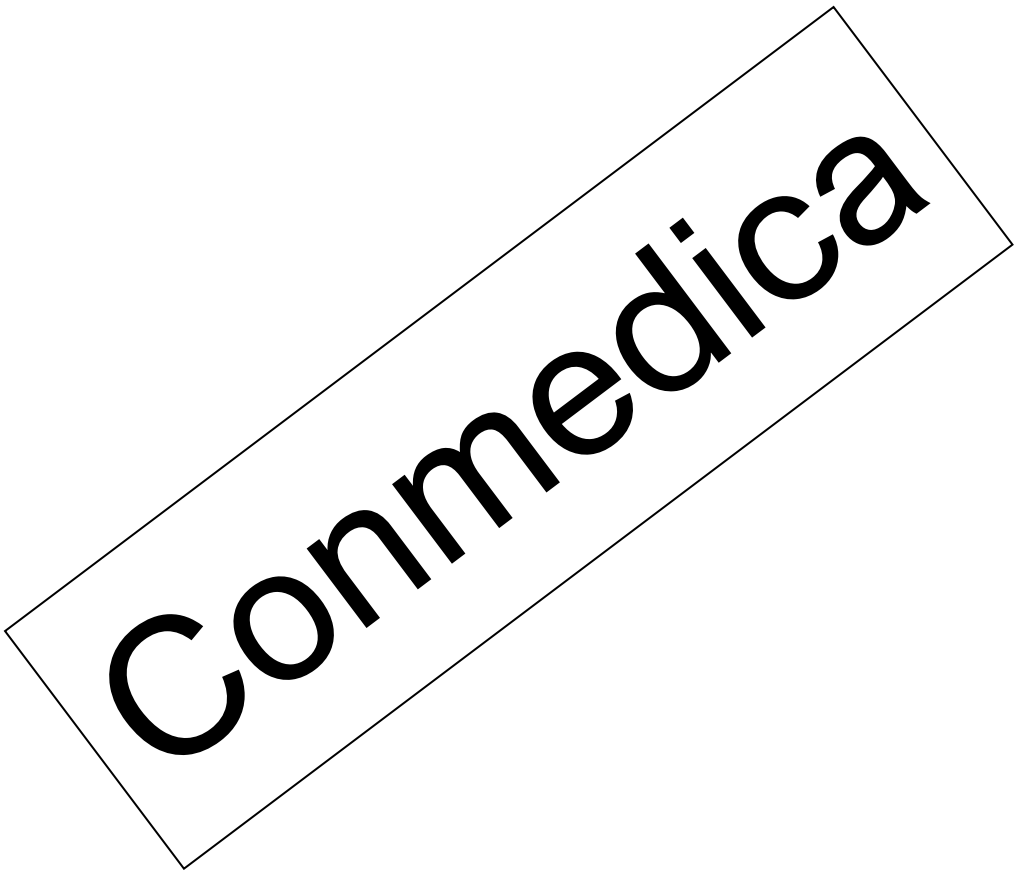
Commedica

Adaptation of left-sided breast deep learning auto-planning model for right-sided breast treatments

Michele Zeverino[1], Raphael Moeckli[1]

[1]*CHUV – Centre Hospitalier Universitaire Vaudois, Lausanne*

Purpose

To develop an auto-planning strategy for right-sided breast treatments by adapting the deep learning-based predicted dose from a pre-existing left-sided breast model.

Methods

The procedure was executed in RayStation v12A TPS and applied to early breast cancer treatments delivering 48Gy/42.4Gy in 16 fractions for PTVBoost and PTVBreast, respectively. Initially, the predicted dose was generated for the right-sided patients using the left-sided model, with swapping of both PTVs and OARs from left to right. Subsequently, the predicted dose underwent post-processing to attain an optimal dose distribution. Finally, the post-processed predicted dose was mimicked using a 2 partial-arcs VMAT technique. The post-processing and mimicking parameters were iteratively adjusted to achieve comparable clinical outcomes for eight manually planned tuning cases. Ultimately, the adapted model was validated against twelve new clinical cases through a planning comparison analysis. Auto-plans treatment geometry and segmentation settings were copied from clinical plans.

Results

In the tuning cases, dose prediction closely matched clinical plans for PTVs (within 3%). However, it overestimated the mean dose for both the heart (+9Gy) and the right lung (+4Gy), the maximum dose to the left lung (+6.5Gy), and the right coronary (+8Gy), and underestimated the maximum dose to the left breast (-4.5Gy). The post-processing was used to reduce the predicted dose for these OARs below their corresponding values of clinical plans accounting for the typical dose deterioration occurring after mimicking. As expected, the mimicking process deteriorated the post-processed predicted dose while maintaining plan quality similar to the clinical cases. During model validation, no significant differences were noted between clinical and auto-plans except for a higher left lung maximum dose (+0.8Gy) and a lower right lung mean dose (-1.2Gy) observed in auto-plans compared to clinical plans.

Conclusion

When applied to right-sided patients, the left-sided auto-planning model's dose prediction required substantial corrections before undergoing mimicking. The post-processing of the predicted dose proved effective in adapting the dose. The auto-planning strategy for right-sided breast treatments was successfully implemented, yielding dose distributions of comparable clinical quality.

DeepSMCP – deep-learning powered denoising of MC dose distributions

Raphael Joost[1], Hannes A. Loebner[1], Jenny Bertholet[1], Stavroula Mougiakakou[2], Michael K. Fix[1], Peter Manser[1]

[1]*Inselspital, Bern University Hospital and University of Bern, Bern*
[2]*ARTORG Center, University of Bern, Bern*

Purpose

To develop a fast, deep-learning based Monte Carlo dose distributions (MCDD) denoising framework for 6, 10 and 15 MV volumetric modulated arc therapy (DeepSMCP) and integrate it into the Swiss Monte Carlo Plan (SMCP).

Methods

DeepSMCP is integrated into the SMCP framework as an additional dose-calculation algorithm and can be selected using the SMCP's graphical user interface. It uses a 4-layer 3D-Unet, to predict a denoised MCDD of low statistical uncertainty, <1% (target), based on the CT and a MCDD of high statistical uncertainty, approximately 60% (input). DeepSMCP is trained on the dose distributions of 106 clinically-motivated VMAT plans for 29 CTs. The plans are augmented to 3074 different plans by randomly changing mu-values, energy (6, 10, 15 MV), collimator-angle and isocenter-position. The number of simulated primary particles is 1.5 MM and 500 MM for input and target dose calculation, respectively. Dose outside the body contour is set to zero. The model denoises 192x192x64 voxels at once. Smaller geometries are padded with zero voxels, larger geometries are handled using a patch-based approach.

Model accuracy is evaluated by gamma passing rate (3% (global)/ 3 mm, 10% threshold) and root-mean-squared error (RMSE) between target and denoised dose distributions for 307 test cases. Model performance is also assessed by calculation time.

Results

Model accuracy shows an average (standard deviation) gamma passing rate of 94.0% (2.3%) and average RMSE of 1.1910-4 Gy/MU (0.2410-4 Gy/MU) for voxels with dose greater 10% of the maximum dose. Model performance on a CPU is on average 32.7 s (7.5 s) for the input MCDD. The subsequent data loading, preprocessing, and denoising takes an average of 2.6 s (0.3 s) on a GeForce RTX 3090 GPU. This compares to a MCDD with low statistical uncertainty taking on average 3.3 h (42 min).

Conclusion

DeepSMCP is successfully integrated into the user-friendly SMCP framework. The introduced approach offers a substantial reduction in computational time compared to a full MC dose calculation, while achieving reasonable accuracy.

Disclosures

Supported by Varian Medical Systems.

Quality assessment of automatically planned O-Ring linac SBRT plans for lung metastases, evaluating the optimal minimum target size

Katerine Viviana Diaz Hernandez[1], Uwe Schneider[1,2], Sergejs Unterkirhers[2]

[1]University Hospital Zurich and University of Zurich, Zurich
[2]Hirslanden Clinic, Zurich,

Purpose

The objective of this study is to assess the feasibility of automated O-Ring Halcyon Linac SBRT plans for lung metastases and determine a Planning Target Volume (PTV) threshold as an indicator of plan quality. The study also contrasts plan quality and treatment durations between Halcyon Linac (HAL) and CyberKnife (CK) robotic SBRT.

Methods

A total of 17 previously treated CK lung treatment plans were automatically generated for the Halcyon system. The prescription doses ranged from 39-54 Gy, with a mean/median of 3 fractions. The mean/median PTV volume was 4.9/4.3 cm³. Plan quality was evaluated using a series of dose target metrics, including New Conformity Index (NCI), Conformity Index (CI), Modified Gradient Index (MGI), spillage, and the percentage of prescribed isodose volume (%PIV). The assessment involved a statistical analysis combining the Wilcoxon rank test and cluster analysis to establish a comparative quality threshold for PTV. The potential impact on organs at risk (OARs) was evaluated based on compliance with international guidelines and predictions of normal tissue complication probabilities (NTCP).

Results

All Halcyon plans and the majority of CK treatment plans (94%, n = 16) adhered to the defined tolerance criteria. Analysis of dosimetric indices demonstrated a statistically significant enhancement in HAL plan quality for target sizes surpassing the found 4.0 cm³ quality threshold. The dose metric of CK plans remained consistently stable across varying PTVs. Notably, only the MGI index exhibited statistically significant inter-cohort differences above the comparative quality threshold. The evaluation of NTCP revealed lung toxicity rates of less than 1.6% for HAL plans and 2.3% for the CK cohort.

Conclusion

Clinical compliance was achieved by all automatically generated Halcyon plans and the majority of CK treatment plans. The identification of a 4.0 cm³ PTV threshold as a predictor for HAL plan quality suggests a potential quality criterion. Further research is essential to validate these observations. It's worth noting that the study did not encompass mechanical limitations and plan delivery assessment, as these aspects were beyond the study's goal.

Dosimetrically motivated collimator angle optimization for linac-based stereotactic radiosurgery of multiple brain metastases

Nathan Torelli[1], Liming Gao[1], Jan Unkelbach[1]

[1]*University Hospital Zurich and University of Zurich, Zurich*

Purpose

The selection of the collimator angle for linac-based stereotactic radiosurgery (SRS) of multiple brain metastases (BMs) is important to reduce the bridge dose in between the different lesions and minimize brain toxicities. In this work, we developed an algorithm which simultaneously optimizes the dose distribution and the collimator angle for SRS of multiple BMs.

Methods

A column generation-based direct aperture optimization algorithm was implemented into our in-house optimization framework. Promising multileaf collimated apertures are iteratively generated for different beam orientations and collimator angles by solving a so-called pricing problem, where dose-influence matrices for apertures at different collimator angles are approximated from the dose-influence matrix at 0° using a rotation function. At each iteration, the aperture with the lowest price is added to the treatment plan and the weights of all apertures in the plan are optimized. The optimization stops when a user-defined number of apertures are generated.

Results

Using the proposed approach, we generated a step-and-shoot non-coplanar IMRT plan for a patient with 29 BMs (with a prescribed PTV dose of 6x5 Gy) and compared the results to an IMRT plan obtained by utilizing a fixed collimator angle at 0° for all apertures. The number of apertures was set to 100 for both plans and the allowed collimator angles ranged from 0° to 175° in 5°-steps. By optimizing the collimator angle, both dose conformity (conformation number: 0.79 vs 0.78) and sparing of the healthy brain (mean brain dose: 6.54 Gy vs 6.81 Gy) could be improved. Several different collimator angles were selected for different beam orientations as well as for the same beam orientation.

Conclusion

A dosimetrically motivated collimator angle optimization method was implemented, which allows to reduce the bridge dose in between the different metastases for SRS-based treatments of patients with multiple BMs. Different from geometrical methods which optimize the collimator angle at each beam orientation by minimizing the island blocking area, multiple optimal collimator angles can be selected for the same beam orientation using the proposed approach.

Development of a workflow to upload treatment plans generated with a research TPS into the commercial Eclipse TPS

Florian Dietsche[1], Nathan Torelli[1], Jan Unkelbach[1]

[1]*University Hospital Zurich and University of Zurich, Zurich*

Purpose

Research treatment planning systems (TPS) are needed for further development of optimization algorithms and exploration of novel concepts not supported by commercial TPS. However, research TPS are not approved medical products and lack the rigorous testing of commercial TPS. In this work, we developed a tool to upload treatment plans generated with our in-house TPS into the Eclipse TPS (Varian Medical Systems).

Methods

Treatment plans generated with our in-house TPS are characterized by a set of multileaf collimator (MLC)-based apertures at different control points. Using the Eclipse Scripting API (ESAPI), treatment plans are created in the Eclipse TPS for the corresponding patient for discrete beam orientations or dynamic arcs, and initialized with control points whose MLC positions are set to the apertures specified in the in-house TPS. Dose distributions for each individual aperture are then computed using Eclipse' commissioned dose calculation algorithms and exported through ESAPI as dose matrices. To mitigate the impact of tongue-and-groove effect, transmission through the MLC and discrepancies between dose calculation algorithms, the fluence of each aperture are re-optimized in the in-house TPS using the exported information. The new monitor unit weights for each aperture are finally uploaded to the Eclipse TPS.

Results

The proposed workflow was tested for a prostate cancer patient. Intensity modulated radiotherapy and volumetric modulated arc therapy treatments generated in the in-house TPS were uploaded to the Eclipse TPS and compared to corresponding plans generated directly in the Eclipse TPS, where the same fields/arcs and same planning objectives were used. The dosimetric quality of the treatments generated in the in-house TPS and Eclipse TPS were similar.

Conclusion

A tool for uploading treatments generated using our in-house TPS into the Eclipse TPS was developed. This potentially enables the clinical delivery of treatment plans that can only be obtained using our in-house research TPS and not directly in commercial TPS. An example are spatiotemporal fractionation schemes, which require the simultaneous optimization of multiple distinct plans based on their cumulative biologically effective dose.

Quality assurance for implementation of online adaptive radiotherapy

Beiqian Qi[1], Térence Risse[1], Geoffroy Guibert[1], Patrick Weber[1]

[1]*Réseau Hospitalier Neuchâtelois, Neuchâtel*

Purpose

The aim of this project is to verify the entire treatment quality of Ethos (Varian, Pola Alto, USA) online adaptive radiotherapy (oART).

Methods

An end-to-end test, specifically designed for oART, was conducted with a water-equivalent 3D printed pelvis phantom. Five organs were included in this phantom: bladder, prostate, rectum and femoral heads. The organs were modeled from the anatomy of a real patient, and simplified to elliptic cylinders. Nine cases of deformation on the bladder, the prostate and the rectum were created with ImSim QA (Oncology Systems Limited, Shrewsbury, UK). The organs were translated, rotated and scaled; the displacement magnitude varied between 0 and 25 mm. These deformed CT images were used for initial planning. For each case, oART was performed with Ethos with prescribed dosimetric goals. The dose delivered to the 3D printed pelvis phantom was measured with a 0.125 cm^3 Semiflex Chamber 31002 (PTW, Freiburg, German) and an EBT3 GafChromic film (Ashland, NJ, USA).

The patient-specific quality assurance (QA) for oART was also verified. The adapted dose calculation was compared between the Ethos treatment planning system and a second dose calculation software Mobius3D (Varian, Pola Alto, USA). The dose delivery of the adapted plans was checked with the ArcCheck phantom (Sun Nuclear, Boulevard, USA).

Results

In the end-to-end test, the single point dose difference was below 2.1% the film measurement showed a 2D gamma passing rate (3%, 2 mm) of 99.2%.

For patient-specific QA, the second dose calculation showed a 3D gamma passing rate (3%, 2mm) higher than 98%; the measurements with the ArcCheck phantom showed a 3D gamma passing rate (3%, 2 mm) above 95%.

Conclusion

A water-equivalent 3D printed phantom was developed for an end-to-end test for oART on Ethos. The dosimetric agreement between the measured dose and calculated dose shows the high quality of treatment adaptation and delivery of Ethos. In conclusion, Ethos oART can be used to treat patients.

Failure modes and effects analysis of the daily adaptive proton therapy workflow at PSI

Katarzyna Czerska[1], Francesca Albertini[1], I Andaca, Evangelia Choulilitsa[1], Frank Emert[1], Filippo Grillo Ruggieri[1], Jan Hrbacek[1], SC Jakobsen[1], Dominic Leiser[1], Antony John Lomax[1], Arturs Meijers[1], S Trosch[1], Miriam Vázquez Varela[1], Damien Charles Weber[1], Michelle van Heerden[1]

[1]PSI – Paul Scherrer Institute, Villigen

Purpose

Daily adaptive proton therapy (DAPT) differs significantly from established processes in conventional radiotherapy. Online adaptation is technologically challenging, needs to be fast and automated and involves new, non-routine steps (e.g., daily plan re-optimization). Therefore, a tailored design of the DAPT workflow, including QA procedures, is required to ensure its safe clinical implementation. To support this, a Failure-Mode-and-Effects-Analysis (FMEA) was performed to proactively identify/quantify risks and integrate mitigation measures into the workflow.

Methods

A multidisciplinary expert team (oncologists/physicists/dosimetrists/therapists) identified potential failure modes (FMs) in the DAPT pre-treatment&online phases, with each FM assigned to a specific category (e.g., imaging). Each FM risk assessment was performed by quantifying its individual severity, probability and detectability {S,D,P} scores, based on (1-10) grading system. Potential effects/causes/mechanisms of each FM, current design control and recommended actions were identified. A few examples were performed together to avoid interobserver variability. Finally, the resulting scores, assigned by team members individually, were discussed and risk priority numbers (RPN=SPD) were calculated for each scenario.

Results

In total, 90 FMs were identified. In both DAPT phases, ~20% of the errors were classified as high-risk (RPN>200; pre-treatment=7, online=13). For these, the current design control and recommended actions were carefully analyzed, verifying also whether the item was DAPT- or PSI-specific. The most frequent FMs, i.e., treatment preparation or calculation/transfer of patient-specific correction vector, were associated with routine treatment steps that could have significantly impact the DAPT process. Human error, either routine or miscommunication, was the most common cause of failure, regardless of the workflow's step.

Conclusions

New technologies, such as DAPT, require proactive risk assessment prior to clinical implementation, not only to ensure safety and development of customized QA-procedures, but also because of the non-existence of error records. Iterative DAPT risk assessment and QA integration has significantly improved the workflow and increased confidence by addressing potential drawbacks, including human-error-type failures. The resulting recommendations (e.g., planQA checks, DAPT-specific procedures) have been implemented and thanks to DAPT-dry-runs, safety of the workflow is tested in live system.

Monte Carlo dose calculation for moving and deforming anatomy

B. Zobrist[1], H.A. Loebner[2], D. Frei[2], W. Volken[2], J. Bertholet[2], M.F.M. Stampanoni[1,3], P. Manser[2], M.K. Fix[2]

[1]Department of Biomedical Engineering, ETH Zurich, Zurich
[2]Inselspital, Bern University Hospital and University of Bern, Bern
[3]PSI – Paul Scherrer Institute, Villigen

Purpose

To develop a deformable voxel geometry (DVG) for Monte Carlo (MC) dose calculation and to integrate it into the Swiss Monte Carlo Plan (SMCP) to account for motion during dose calculation of radiotherapy treatment plans by deforming the patient geometry.

Methods

A volumetric modulated arc plan is created for a non-small cell lung cancer case (without breathing, static situation). Additionally, deformation vector fields (DVF) to account for the breathing motion are calculated using the B-splines image registration of plastimatch based on the 4DCT. The DVFs are used to deform the DVG during the Monte Carlo dose calculation. The resulting dose distribution considering the breathing motion is compared to the dose distribution without breathing motion.

To validate the DVG for rigid motion, the plan is delivered to a Delta4 phantom on a TrueBeam in developer mode. Continuous anterior-posterior couch motion (amplitude 5 cm) is moving the phantom during beam-on. The calculation of the dose distribution includes the couch movements by dynamically deforming the voxel geometry accordingly. The calculated dose is compared to the measured one.

Both dose comparisons are done by means of dose differences and gamma passing rate (GPR) (3% (global)/2 mm, 10% threshold).

Results

The dose distribution considering the breathing motion agrees by 86.8% GPR with the static situation. In the target volume they agree by 69.1% GPR. Breathing motion deteriorates the planned dose by up to 35% of the local dose, with the greatest dose differences observed in high dose gradient regions. The validation measurement agrees by 99.3% Gamma Passing Rate with the calculated dose which accounts for the motion.

Conclusion

A deformable voxel geometry for MC dose calculation is successfully developed for the SMCP framework, to account for motion during dose calculation. It is validated for rigid motion during dose calculation.

Disclosures

Supported by Varian Medical Systems.

Monte Carlo model of an ETHOS radiotherapy beam

Michael K Fix[1], Werner Volken[1], Daniel Frei[1], Daniel Schmidhalter[1], Peter Manser[1]

[1]*Inselspital, Bern University Hospital and University of Bern, Bern*

Purpose

To implement, commission and validate a Monte Carlo (MC) model of an ETHOS radiotherapy beam within the Swiss Monte Carlo Plan (SMCP).

Methods

The geometry and material of the treatment head model consisting of the target, the primary collimator, the monitor chamber, the secondary collimator and the double-stack multi-leaf collimator (MLC) was implemented into SMCP following the information provided by the vendor. For the commissioning, parameters for the Gaussian shaped position and direction distributions as well as for the energy spectrum of the initial primary electron beam impinging on the target were tuned in order to match measured dose distributions. For this purpose, depth dose curves and lateral dose profiles in five depths ranging from 1.3 cm to 15 cm were measured for square MLC shaped field sizes ranging from 1 x 1 cm to 28 x 28 cm at a source to surface distance (SSD) of 100 cm in units of cGy/MU. For the validation the analogous set of dose values at SSD of 90 cm were measured and compared with the corresponding calculated dose distributions using the commissioned MC model. In addition, a complex irregular shaped MLC field (fish-bone) with MLC leaf openings down to 2 mm were measured with a radiochromic film in a depth of 5 cm of a solid water phantom at SSD of 95 cm and compared with the corresponding MC dose calculation.

Results

An MC model of the ETHOS radiotherapy beam was successfully implemented in SMCP. The commissioned MC model agreed in general within 1% (global) or 1 mm for all depth dose curves and lateral dose profiles in units of cGy/MU for all square field sizes considered. For the fish-bone shaped complex MLC field dose differences of up to 5% (in regions with a large dose gradient) or 1 mm were observed.

Conclusion

A commissioned and validated MC model of an ETHOS radiotherapy beam is now available in the SMCP framework for accurate dose calculations.

Disclosures

Supported by Varian Medical Systems.

Validation of a 6 MV flattening filter free phase space of a C-arm linear accelerator for a Monte Carlo framework

Francine El Khoury Youhanna[1], Michael Fix[2], D. Frei[2], Gian Guyer[2], Peter Manser[2], Silvan Müller[2], Marco Stampanoni[1,3], W. Volken[2]

[1]Department of Biomedical Engineering, ETH Zurich, Zurich
[2]Inselspital, Bern University Hospital and University of Bern, Bern
[3]PSI – Paul Scherrer Institute, Villigen

Purpose

To validate a 6 MV flattening filter free (FFF) phase space, determined in previous works, of a TrueBeam system for a Monte Carlo (MC) dose calculation framework.

Methods

The 6 MV FFF phase space, scored at the end of the patient-independent part (above the secondary collimator jaws), is used to calculate MC dose distributions inside a water phantom for square, rectangular, off-axis and MLC collimated fields and two volumetric modulated arc therapy (VMAT) plans consisting of 4 and 6 arcs, respectively. The dose distributions of the open fields were measured inside a water bath using a Semiflex 3D and a microDiamond detector (PTW, Freiburg, DE). The depth dose (DD) curves, X-profiles and Y-profiles of the absolute dose distributions were compared using a 1D gamma analysis, with a 1% (global), 1 mm criterion. The dose distributions of the VMAT plans were measured using radiochromic films and compared to the MC calculated dose distributions using a 2D gamma analysis, with a 3% (global), 2 mm criterion and a 20% low-dose threshold.

Results

The gamma passing rate between the (Semiflex 3D) measured and MC calculated dose distributions averaged at 92% (56%-94%) for DD curves, 98% (27.27%-100%) for X-profiles and 96% (27.3%-100%) for Y-profiles for all depths. The disagreement being mainly in the build-up region of the DD curves, where the calculated dose is lower than the measured dose. Comparing measurements performed with the microDiamond detector and the MC calculated DDs, the gamma passing rate averaged at 99.9% (99.35%-100%) for PDDs, 96% (76.36%-100%) for X-profiles and 95 % (74.1%-100%) for Y-profiles for all depths. For the VMAT plans, the gamma passing rates between the measured and MC calculated dose distributions were 95% for the 4 arcs case and 99% for the 6 arcs case.

Conclusion

A phase space for a 6 MV FFF photon beam of a TrueBeam system was successfully validated for open and intensity-modulated fields.

Monte Carlo codes for very high energy electrons: dosimetric and calculation time comparison

Chengchen Zhu[1], Jenny Bertholet[1], Michael Fix[1], Gian Guyer[1], Hannes Loebner[1], Peter Manser[1], Silvan Müller[1], Marco Stampanoni[2,3], Werner Volken[1]

[1]Inselspital, Bern University Hospital and University of Bern, Bern
[2]PSI – Paul Scherrer Institute, Villigen
[3]Department of Biomedical Engineering, ETH Zurich, Zurich

Purpose

To develop a versatile dose calculation framework for very high energy electron (VHEE) beams on patient CTs using various Monte Carlo (MC) codes and to compare their dose distributions and calculation times.

Methods

MC dose distributions of mono-energetic electron beams with energies 10-250 MeV, defined by a rectangular shape (10 x 10 cm2, parallel incidence) and impinging frontally onto a patient's chest are calculated. VMC++, EGSnrc, Geant4 using option EMZ, and Geant4 using option PENELOPE are used for dose calculation. Each calculation considers ten million particle histories (statistical uncertainty <1.5%) and runs parallelly on 10 CPUs (Ubelix HPC Cluster, AMD EPYC 7742, 2.25 GHz). Dose distributions are compared per energy using integrated depth-dose curves and lateral-dose profiles normalized to dose maximum. Total calculation times are logged.

Results

Dose maximums range between 4.1-17.1 cm inside the patient for energies up to 100 MeV and locate at the beam exit from the patient (22.7-23.2 cm) for higher energies. Integrated depth-dose curves from different MC codes agree within 4.6% (global), with the greatest difference between Geant4-EMZ and VMC++ for 40 MeV. Integrated lateral-dose profiles agree within 1.3% (global) with the largest difference between Geant4-EMZ and VMC++ for 20 MeV. The differences occur at interfaces of different tissues (e.g., ribs and lung-tissue).

Computation times range between 0.1-0.2 h (VMC++), 3.5-10.7 h (EGSnrc), 11.2-25.0 h (Geant4-EMZ), and 13.3-28.1 h (Geant4-PENELOPE). Calculation time increases rapidly for energies below 70 MeV and slowly for higher energies for VMC++ and EGSnrc. For both Geant4 options, calculation times for 110-250 MeV are shorter by a maximum of 43% compared to the longest calculation time (100 MeV), likely due to limited patient thickness and electrons exiting the geometry without interacting.

Conclusion

An MC framework for VHEE dose calculations on patient CTs with different MC codes was successfully developed. Substantial dose differences at tissue interfaces and shorter calculation times at higher energies with Geant4 options are resulted for the considered case.

Disclosures

This work was supported by Varian Medical Systems.

Post Y-90 radioembolization patient image quality and dosimetry evaluation with whole-body Biograph Quadra PET/CT

Konstantinos Zeimpekis[1], Lorenzo Mercolli[1], Axel Rominger[1], Hendrik Rathke[1]

[1]*Inselspital, Bern University Hospital and University of Bern, Bern*

Purpose

Whole-body PET/CT Biograph Quadra with a AFOV of 106 cm, offers higher sensitivity compared to a standard AFOV scanner. Taking advantage of this, we evaluate the image quality, tumor absorbed dose and lung dose in patients post-radiomebolization with Y-90.

Methods

17 Patients were scanned with a median injected activity of 2.3 +/- 1.2 GBq on a Siemens Biograph Quadra (Siemens Healthineers, Knoxville, TN, USA). The original scan time was 20 minutes and 1, 5, 10 and 15 minute list-mode date were reconstructed as well. The image quality assessment was done in terms of lesion SNR and background noise using VOIs on syngo.via. Dosimetry evaluation was done on HERMES. Wilcoxon signed rank test was used for statistial significance with a p-value<0.05.

Results

Lesion SNR: No difference of statistical significance from 20 down to 10 minutes reconstructed time. Noise: Similarly down to 5 minutes. Dosimetry: assessment of mean lung absorbed dose lower than the planned for all reconstucted times. Tumor absorbed dose: No difference of statistical significance from 20 down to 5 minutes reconstructed times.

Conclusion

Though a preliinary evaluation, 10 minutes seem a feasible scan time for patients after Y-90 radioembolization for post-treatment localization and treatment dosimetry. This can lead to an optimized patient throughput due to shorter scan times and patient comfort.

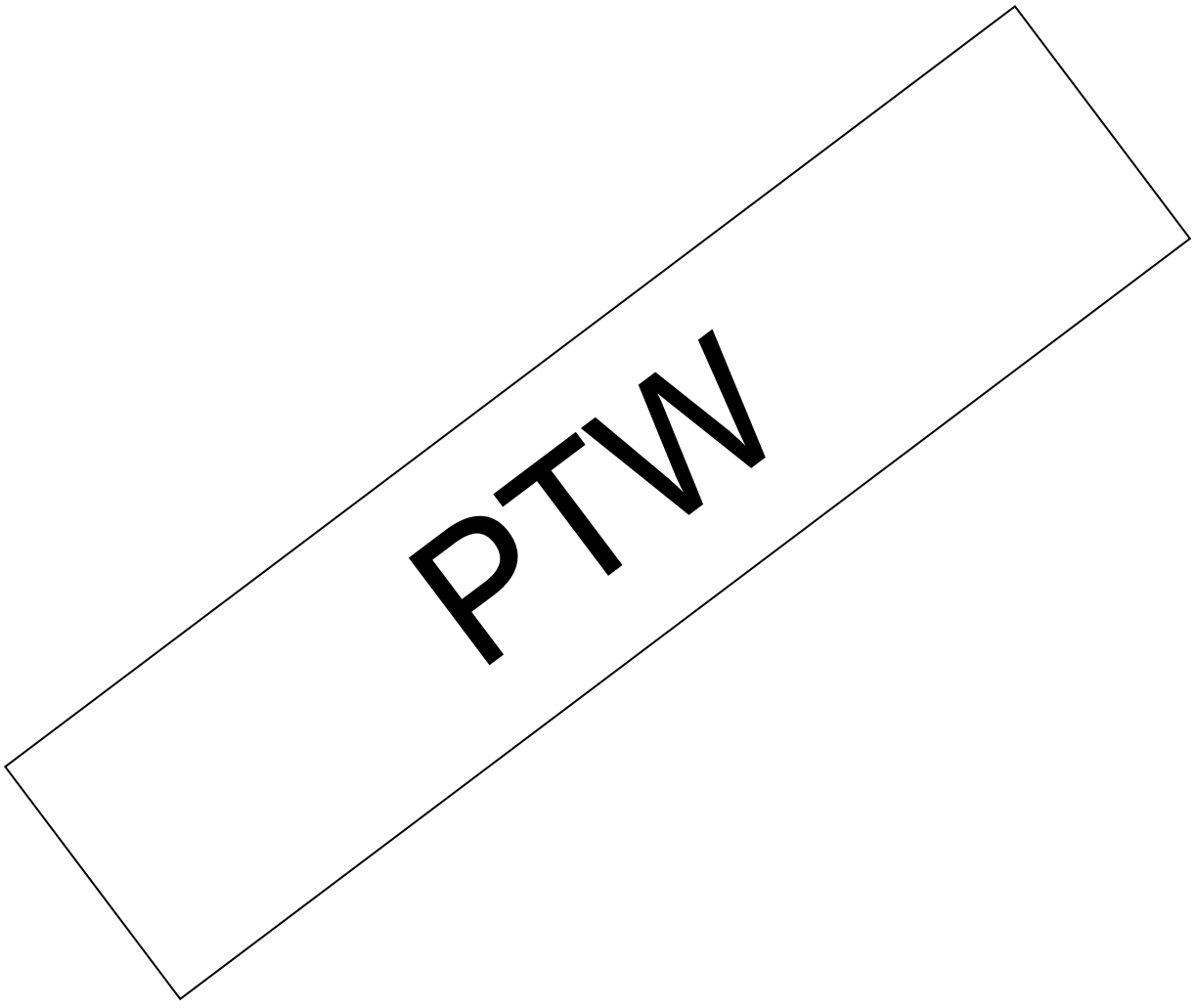
PTW